

Lawrence Berkeley National Laboratory

Recent Work

Title

TANTALUM SPALLATION AND FISSION INDUCED BY 340-M PROTONS

Permalink

<https://escholarship.org/uc/item/5dz2g550>

Author

Nervik, W.E.

Publication Date

1954-04-07

UCRL—2542

UNCLASSIFIED

UNIVERSITY OF
CALIFORNIA

*Radiation
Laboratory*

TWO-WEEK LOAN COPY

*This is a Library Circulating Copy
which may be borrowed for two weeks.
For a personal retention copy, call
Tech. Info. Division, Ext. 5545*

BERKELEY, CALIFORNIA

DISCLAIMER

This document was prepared as an account of work sponsored by the United States Government. While this document is believed to contain correct information, neither the United States Government nor any agency thereof, nor the Regents of the University of California, nor any of their employees, makes any warranty, express or implied, or assumes any legal responsibility for the accuracy, completeness, or usefulness of any information, apparatus, product, or process disclosed, or represents that its use would not infringe privately owned rights. Reference herein to any specific commercial product, process, or service by its trade name, trademark, manufacturer, or otherwise, does not necessarily constitute or imply its endorsement, recommendation, or favoring by the United States Government or any agency thereof, or the Regents of the University of California. The views and opinions of authors expressed herein do not necessarily state or reflect those of the United States Government or any agency thereof or the Regents of the University of California.

Unclassified-Chemistry Distribution

UNIVERSITY OF CALIFORNIA

Radiation Laboratory

Contract No. W-7405-eng-48

TANTALUM SPALLATION AND FISSION INDUCED BY 340 MEV PROTONS

Walter Edward Nervik

(Thesis)

April 7, 1954

Berkeley, California

TABLE OF CONTENTS

	Page
ABSTRACT	3
Part	
I. INTRODUCTION	4
II. EXPERIMENTAL PROCEDURES	8
A. Target Arrangements	8
B. Treatment of the Target After Bombardment	12
C. Chemical Procedures	14
III. RADIOACTIVE NUCLIDES OBSERVED	39
A. Resolution of Decay Curves	39
B. Calculation of Disintegration Rates	43
C. Calculation of Cross Sections	49
D. Nuclides Observed	50
IV. RESULTS AND DISCUSSION	81
V. ACKNOWLEDGMENTS	98
VI. REFERENCES	99

TANTALUM SPALLATION AND FISSION INDUCED BY 340 MEV PROTONS

Walter Edward Nervik
Radiation Laboratory and Department of Chemistry
University of California, Berkeley, California

April 7, 1954

ABSTRACT

Tantalum metal was irradiated with 340 Mev protons in the 184-inch cyclotron. Nuclides formed as spallation and fission products during the bombardments were separated chemically, identified, and their formation cross sections calculated. A very broad fission peak which extended from mass 20 to mass 132 was observed. The maximum fission yield occurred in the region of the nuclide Kr^{83} and analysis of a set of contour curves fitted to the data indicated that either Hf^{166} or Lu^{166} was "the most probable fissioning nucleus." The total cross section for fission was estimated to be 4.1 mb. Comparison of the fission data of tantalum with that of uranium and bismuth under the same bombardment conditions indicated that asymmetric fission was much more probable in tantalum than in either of the other elements. In the spallation region it was observed that neutron emission was the predominant spallation reaction. Integration under the spallation yield curve indicated that of those tantalum target nuclei which received at least enough excitation energy to reach the region of "the most probable fissioning nucleus" less than 1 percent underwent fission; the remainder emitted spallation fragments.

TANTALUM SPALLATION AND FISSION INDUCED BY 340 MEV PROTONS

Walter Edward Nervik
Radiation Laboratory and Department of Chemistry
University of California, Berkeley, California

April 7, 1954

I. INTRODUCTION

Ever since machines became available which would accelerate charged particles to high energies considerable interest has been shown in the mechanism of fission and the distribution of fission products induced by those particles.

The earliest fission product studies, and the reaction on which the most complete data are available, concerned the thermal neutron fission of uranium. Principal features of this fission process are:

1. Predominantly asymmetric splitting of the compound nucleus as shown by the appearance of two peaks in the fission yield versus mass curve.
2. Essentially complete absence of fission products on the neutron deficient side of stability.
3. Extremely steep slopes on both "wings" of the fission yield versus mass curve, with no fission products having a mass less than 72 or greater than 162 being observed in abundances greater than 10^{-5} percent of the fission events.

As the incident neutron energy is increased the shape of the fission yield versus mass curve begins to change markedly, particularly in the region of symmetrical fission. Engelkemeir^{1,2} and co-workers observed that when Pu²³⁹ was irradiated with neutrons of

approximately 600 kev the yield of Pd^{109} was 50 percent higher than the yield with thermal neutrons. Turkevich and Niday,³ bombarding thorium with pile neutrons of 2.6 Mev average energy, also observed an increase in the symmetrical fission region and suggested that the fission process at these energies is a combination of two types, one asymmetric and the other symmetric.

When the neutron energy is increased still further the probability of symmetrical fission becomes even more pronounced. Spence⁴ has shown that when U^{235} is irradiated with 14 Mev neutrons, symmetrical fission becomes one hundred times more probable than with thermal neutrons. Also, this rise in the symmetrical fission yield was accompanied by a decrease in the yields of those nuclides which lay at the peaks of the thermal neutron yield curve; i.e., the yield of Mo^{99} was about 15 percent lower at 14 Mev than with thermal neutrons.

This increase in the symmetrical fission probability at higher excitation energies has also been observed in charged particle bombardments. Newton,⁵ irradiating thorium with 37.5 Mev alpha particles, showed that the symmetrical fission yield is almost equal to that for asymmetrical fission and that the deep minimum in the yield curve for the thermal neutron fission of U^{235} had practically disappeared. Here the compound nucleus is the same for both particles so that direct comparison of the two yield curves is justified. When bombarding energies are increased to extremely high values (i.e., uranium with 380 Mev alpha particles⁶) symmetrical fission predominates and the yield versus mass curve shows a single peak with no perturbations for asymmetric fission.

This single symmetrical fission peak has also been observed when elements lighter than uranium or thorium were bombarded with very high energy particles. Goeckermann and Perlman,⁷ bombarding bismuth with 190 Mev deuterons, observed this type of fission peak. In addition, they noted that the maximum of the symmetric fission peak corresponded to a mass less than half the mass of the target nucleus. Their conclusion was that twelve nucleons had evaporated before fission occurred. Furthermore, the peaks of their isobaric chain yields indicated that most of the chain yield for a given mass number was concentrated in the nuclide having the same neutron to proton ratio as the fissioning nucleus.

Progressing still farther down the periodic table, fission has been observed for a number of medium weight elements. Batzel and Seaborg,^{8,9} irradiating copper, bromine, silver, tin, and barium with very high energy protons, separated activities which lay in the region of the periodic table corresponding to roughly symmetrical fission for each of these elements. Proof that fission and not spallation of alpha particles was actually occurring in these bombardments was based primarily on the observed thresholds and calculated energetics of the reactions involved. Thus the calculated threshold for the spallation reaction $\text{Cu}^{63}(\text{p}, \text{p}_3 \text{n} \alpha) \text{Na}^{24}$ was about 170 Mev while the threshold for the fission reaction $\text{Cu}^{63} + \text{p} = \text{Na}^{24} + \text{K}^{39} + \text{n}$ was approximately 50 Mev. Since Na^{24} was produced in 70 Mev proton bombardments of copper, the conclusion was drawn that it must have been formed by a fission process.

Evidence for fission of the medium weight elements in the references quoted was based on radiochemical separation of only a few of the possible activities formed. As part of a program of assembling detailed information showing how a single particle of a single energy reacts with widely differing target elements iron,¹⁰ nickel,¹¹ copper,⁸ zinc,¹² silver,¹³ bismuth,¹⁴ and uranium,^{15,16} have been bombarded with 340 Mev protons in the Berkeley cyclotron. Radiochemical separation and identification of activities formed in both the spallation and fission regions was carried out. These data indicate that for the five light elements spallation is by far the most prevalent reaction, with highest yields on the neutron deficient side of stability near the target nucleus. In the binary fission region the yields are very low and the yield versus mass number curves are merely a flattened extension of the spallation portion of the curve. It should be mentioned that although yields in the fission region for these elements are low they are measurable, and every element below the target element is formed in some degree during this type of bombardment.

For bismuth and uranium, fission is the predominant reaction and the characteristic single symmetrical high energy fission peak is obtained. In each case the fission peak height and the chain yield distributions are such as to indicate initial evaporation of nucleons followed by a fission process in which the neutron to proton ratio of the fissioning nucleus is preferentially maintained in the fission fragments.

The present work on tantalum was undertaken as part of this over-all program of 340 Mev proton bombardments. Tantalum was of particular interest in this series because of its position in the periodic table. Because of the mass defect, atoms of heavy elements like thorium or uranium are strongly exoergic toward fission. Light elements like copper are thermodynamically much more stable, however, and a larger excitation energy must be imparted to the nucleus for fission to occur. The result is that only a very small fraction of reactions in the copper bombardments yield products which may be considered as fission fragments. Tantalum lies between these two extremes, and while it was expected that the total fission cross section would be low there was some question as to whether or not a fission peak would be discernable.

It should be noted that in previous work in this program spallation data for the five lighter elements was rather complete and the fission data meager, while for bismuth and uranium the opposite was true. It was hoped that the tantalum bombardments would yield enough data on both spallation and fission to enable more accurate conclusions on the mechanism of those reactions to be drawn.

II. EXPERIMENTAL PROCEDURES

A. Target Arrangements

The target material used in this series of experiments consisted of the purest tantalum foil available. Spectrographic analysis of the metal showed it to be free of any impurities which

might interfere with the fission product yields except for approximately 0.01 percent of niobium. Spallation yields for middle weight elements indicated that this impurity would probably affect only the neutron deficient nuclides of molybdenum, niobium, zirconium, and strontium in the fission product region of tantalum. The remaining fission product activity and all of the activities in the spallation region had to be formed from tantalum in these bombardments.

In order to measure the absolute cross section of the spallation and fission products the proton beam monitoring procedure developed by Folger and Stevenson¹⁵ was followed. One inch diameter disks were cut out of 0.00025 inch aluminum, 0.001 inch aluminum, and 0.002 inch tantalum foil with the same die to ensure that they all had the same area. Surface impurities were removed by washing the aluminum disks in conductivity water and acetone and drying in an oven. The tantalum disks were cleaned in hot concentrated nitric acid, rinsed in conductivity water and acetone and dried.

Si-Chang Fung¹⁷ has shown that in bombardments with 340 Mev protons a significant fraction of the activity formed in a quarter mil aluminum foil may be lost through recoil but that this loss could be minimized by placing one mil aluminum "guard foils" in front and back of the thinner foil. In addition, since recoiling atoms from the copper target holder might introduce contaminating activities in the region of copper into the tantalum target foils, a two mil tantalum "guard foil" was placed in front and back of the tantalum target foils. Thus the target "sandwich" consisted of one

mil Al guard, quarter mil Al monitor, one mil Al guard, two mil Ta guard, Ta target (usually three two mil Ta disks), two mil Ta guard, one mil Al guard, quarter mil Al monitor, and one mil Al guard. The sandwiched disks were aligned exactly, clamped firmly in the copper target holder, and trimmed about a quarter inch from the face of the target holder. A scale diagram of this "Thin Target" arrangement is shown in Figure 1.

After bombardment the monitor foils were weighed and mounted and their decay followed. The 15 hour activity of Na^{24} could easily be resolved from the decay curve. Since the formation cross section for the $\text{Al}^{27}(\text{p},3\text{pn})\text{Na}^{24}$ reaction was known, the cross sections for the spallation and fission products in tantalum could be calculated.

After several "Thin Target" bombardments had been evaluated it became apparent that not enough activity was being formed in the fission product region for good statistical counting and accurate resolution of the gross decay curves. Recourse was taken to the "Thick Target" arrangement in which a stack, usually six, of two mil x 0.25 inch x 1.75 inch tantalum target foils was wrapped in one thickness of two mil Ta guard foil and clamped in a copper target holder in such a manner that the proton beam traversed the 0.25 inch dimension of the target. Nickel was used as the "internal monitor" on each of the thick target bombardments. Since the cross section for the reaction $\text{Ta}^{181}(\text{p},\text{fission})\text{Ni}^{66}$ had been calculated from the thin target bombardments, the cross section for all of the fission products could be obtained by comparing their activities to that of Ni^{66} .

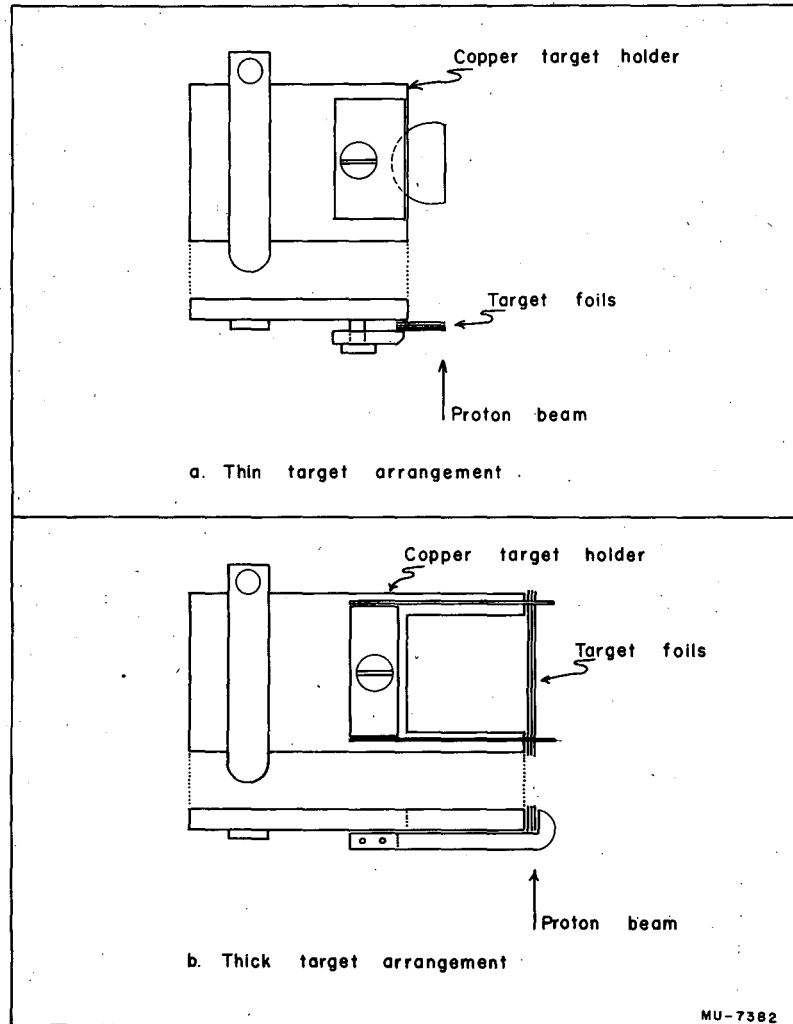


Figure 1. Target foil arrangements.

B. Treatment of the Target After Bombardment

After data from preliminary experiments had been assembled it became apparent that chemical treatment of the target after bombardment had to be governed by several equally important factors:

1. Fission product cross sections were extremely small, being approximately 10^{-4} that of the spallation cross sections. Thus radiochemical purification factors of about 10^7 were required between the fission product activities and those in the spallation region (W, Ta, Hf, and the rare earths).

2. Activities of every element below the rare earths were present in comparable yields. Radiochemical purification factors of approximately 10^4 were required between each of the fission product elements and all of the elements below the rare earths.

3. Tantalum is a notoriously difficult metal to get in solution. It will dissolve easily only in a mixture of concentrated hydrofluoric acid and concentrated nitric acid. Chemical separation procedures all had to begin with this HF-HNO₃ solution.

4. Activity levels of the fission products, even with the thick target arrangements, were so low that the original target solution could not be separated into aliquots. Thus all of the elements which were to be separated in one bombardment had to come out of the entire original target solution.

With these factors in mind, the radiochemical separation procedures were developed. Exact procedures for each element will be described subsequently, but in general the target material was

dissolved in concentrated HF-HNO₃. Accurately known quantities, usually 10 mg, of the elements to be separated were added and the elements separated and purified. Assuming complete exchange between the active atoms and the inert carrier atoms in the original solution, the weight of the carrier recovered at the completion of the purification would determine the fraction of the original activity recovered. In several elements special steps had to be taken to ensure complete exchange. In others, where there was danger of the active atoms being adsorbed on the walls of the lusteroid cones in which the target was dissolved before the inert carrier could be added, the carrier had to be added before the target was dissolved. In any case the carriers were added as soon as practicable.

The final purified compound was transferred wet to a tared aluminum dish which had a depression of 1 cm² area to define the area of the final compound. After drying and weighing, a drop of dilute clear lacquer was placed on the precipitate and dried. This material did not contribute significantly to the mass of the sample and yet served to bind the sample in place during the subsequent counting operations. Those compounds which could not be dried adequately in aluminum were first ignited in porcelain or platinum crucibles and the dried powders transferred to the tared aluminum dishes. For counting purposes the final weighed samples were fastened to 2 mm thick aluminum mounting plates which held the dishes in a fixed position and were constructed to fit the shelving arrangement of the various counters.

C. Chemical Procedures

Obviously, when radiochemical separation procedures are being developed for a fission yield study of this type, the separation techniques commonly in use will be adapted wherever possible. Thus some of the procedures given here are but slight modifications of well-known operations. In a number of cases, however, the separation requirements were such that previously published procedures were either completely inadequate or impossibly impractical. New separation techniques had to be devised. Therefore the procedures for tungsten, hafnium, zirconium, tantalum, the rare earths, indium, rhodium, cesium, rubidium, potassium, chromium, and magnesium represent either major modifications of existing procedures or completely new ones developed especially for these bombardments.

The primary requirement for these chemical procedures is maximum purity in a minimum time. In addition, since the thick targets usually had from three to five hundred roentgens of activity at a distance of two inches when the chemical steps were begun, the question of minimum exposure for the chemist had to be considered. When possible, the spallation products (Ta, Hf, rare earths) were separated first in order to lower the general activity level, then the desired elements were separated. Scavenging agents for any but the spallation elements were seldom added until the desired element had been removed from the target solution. All chemical separations (at least until the activity decreased to a safe level) were performed with three foot long tongs passed through slots in a four inch thick lead brick wall, the whole built into a standard ventilating

hood. When necessary because of especially high activity levels, operations behind the lead wall were observed by means of strategically placed mirrors.

Sodium:--The Ta target was dissolved in concentrated HF-HNO₃ and sodium carrier added. Cerium carrier was added to precipitate the rare earth fluoride and hafnium and barium carrier to precipitate BaHfF₆. The precipitates were centrifuged, the solution made 18 N in H₂SO₄ and tantalum extracted with di-isopropyl ketone. The aqueous layer was evaporated to dryness in a platinum vessel, the residue dissolved in water, copper carrier added, H₂S passed through the solution, and the acid-insoluble sulfides centrifuged. After boiling to destroy the H₂S, Ba, Sr, and Fe carriers were added, the solution made basic with NH₄OH, (NH₄)₂CO₃ added, and the ammoniacal insoluble hydroxides and carbonates centrifuged. Nickel was precipitated with dimethylglyoxime and separated by filtration. Concentrated HNO₃ was added and evaporated almost to dryness. Concentrated perchloric acid, potassium, rubidium, and cesium carriers were added and evaporated almost to dryness. The solution was chilled and Na leached out of the perchlorate precipitate with ice cold ethyl acetate. Water was added to the ethyl acetate and evaporated almost to dryness. Zinc uranyl acetate solution was added, chilled, and the sodium zinc uranyl acetate precipitate centrifuged. The precipitate was dissolved in a minimum volume of concentrated HCl and ice cold isopropyl alcohol saturated with HCl gas was added. The NaCl was washed with HCl-saturated isopropyl alcohol and dissolved in H₂O. The CuS, Fe(OH)₃ scavenges were repeated. Concentrated HClO₄ was added, evaporated to dryness, heated

until any ammonium salts had been destroyed, and the residue dissolved in water. The sodium zinc uranyl acetate and sodium chloride precipitations were repeated. The final NaCl precipitate was washed three times with HCl-saturated isopropyl alcohol, dried at 115° C and weighed as NaCl.

Magnesium:--Magnesium carrier was added to the tantalum target solution. Cerium carrier was added and the rare earth fluorides centrifuged, the solution made 18 N in H₂SO₄, and tantalum extracted with di-isopropyl ketone. The aqueous layer was evaporated almost to dryness and the residue dissolved in water. Iron carrier was added, the solution made basic with NH₄OH (the volume had to be large or magnesium would have carried down on the ferric hydroxide), and the ammoniacal insoluble hydroxides centrifuged. Copper carrier was added and the basic insoluble sulfides precipitated with H₂S. The solution was adjusted to pH 4 with acetic acid, 1 mg Ca, Sr, Ba carriers and 1 ml of saturated oxalic acid solution added, and the acid insoluble oxalates centrifuged. The oxalate scavenge was repeated twice. The solution was evaporated almost to dryness, concentrated HNO₃ added and boiled to destroy C₂O₄²⁻. Diluted with water, the solution was made basic with NH₄OH, (NH₄)₂HPO₄ solution added, the magnesium ammonium phosphate precipitate centrifuged and washed with dilute ammonia. The precipitate was dissolved in a minimum volume of concentrated HCl, diluted to approximately 0.1 M and passed through a 2 mm x 10 cm Dowex-50 cation exchange resin column. (Magnesium was adsorbed and the phosphate passed through.) The column was washed with water and the magnesium stripped off with

6 N HCl. The $\text{Fe}(\text{OH})_3$, CuS , and CaC_2O_4 scavenges, the phosphate precipitation, and the column separation were repeated. The final 6 N HCl solution was evaporated almost to dryness, diluted with water, made basic with NH_4OH , $(\text{NH}_4)_2\text{HPO}_4$ solution added, and the $\text{Mg}(\text{NH}_4)\text{PO}_4$ centrifuged. The precipitate was twice washed with water, twice with ethanol, ignited at 1300°F and weighed as $\text{Mg}_2\text{P}_2\text{O}_7$.

Potassium:--Potassium and cerium carriers were added to the Ta target solution, the rare earth fluorides centrifuged, the solution made 18 N in H_2SO_4 , Ta extracted with di-isopropyl ketone, and the aqueous layer evaporated almost to dryness in a platinum vessel. The residue was dissolved in water, Cu carrier added, H_2S passed in, and the acid insoluble sulfides centrifuged. After boiling to expel H_2S , Fe, Ba, Sr carriers were added, the solution made basic with NH_4OH , $(\text{NH}_4)_2\text{CO}_3$ added and the basic insoluble hydroxides and carbonates centrifuged. Nickel was precipitated with dimethylglyoxime and the solution filtered. Concentrated HNO_3 was added and evaporated almost to dryness. Rubidium, cesium carriers, concentrated HClO_4 were added and evaporated almost to dryness. The cooled perchlorate precipitate was washed with ice cold ethyl acetate and heated to expel excess ethyl acetate. After the KClO_4 was dissolved in water and the CuS and $\text{Fe}(\text{OH})_3$ scavenges repeated, the solution was evaporated to dryness and heated to vaporize ammonium salts. Concentrated HClO_4 was added, evaporated to dryness, cooled, and the residue washed with ice cold ethyl acetate. The perchlorates were dissolved in water and the solution passed through a 10 mm x 7 cm Duolite C-3 phenol formaldehyde type cation exchange resin column which was in its acid form (K, Rb,

and Cs were adsorbed). After washing the column with water, potassium was eluted with 0.1 M HCl solution. With this acid concentration potassium would be eluted first, rubidium and cesium being far behind. Evaporating the potassium fraction to dryness, concentrated HClO_4 was added and evaporated almost to dryness again. Cooled, the precipitate was washed three times with ethanol, dried under a heat lamp and weighed as KClO_4 .

Chromium:--Chromium and cerium carriers were added to the Ta target solution, the rare earth fluorides centrifuged, the supernatant made approximately 8 N in HCl, and Ta extracted with di-isopropyl ketone. The aqueous layer was evaporated to dryness, cooled, concentrated HClO_4 added, and chromium distilled in a stream of HCl gas, the distillate being collected in ice cold water. To the distillate H_2O_2 and Fe carrier were added, the solution made basic with NH_4OH , and the basic insoluble hydroxides centrifuged. After neutralizing the solution, Ba carrier was added and the BaCrO_4 centrifuged. The BaCrO_4 was dissolved in HCl, As, Sb, and Pd carriers added, H_2S bubbled, and the acid insoluble sulfides centrifuged. The BaCrO_4 was transferred to a distilling flask, Ru carrier and concentrated HClO_4 added, and the solution heated to expel the RuO_4 . After cooling and neutralizing the solution with NH_4OH , Ba carrier was added and the BaCrO_4 precipitate centrifuged. The precipitate was transferred into a separatory funnel, ethyl ether, 30 percent H_2O_2 were added, and the blue chromium complex extracted. Chromium was back extracted with dilute NH_4OH . The solution was scavenged with $\text{Fe}(\text{OH})_3$. After neutralizing, Ba carrier was added, The BaCrO_4 was

centrifuged, washed twice with water, twice with ethanol, dried at 110° C, and weighed as BaCrO_4 .

Manganese;--The target was dissolved in the presence of the manganese carrier. Cerium carrier was added, the rare earth fluorides centrifuged, the solution made 18 N in H_2SO_4 , tantalum extracted with di-isopropyl ketone, and the aqueous layer evaporated almost to dryness. After the residue had been dissolved in 1 M HNO_3 , a slight excess of KBrO_3 was added, the solution boiled to coagulate MnO_2 , centrifuged, and the precipitate washed with 1 M HNO_3 . The MnO_2 was dissolved in concentrated HCl and the concentrated HCl solution passed through a $2 \text{ mm} \times 5 \text{ cm}$ Dowex A-2 anion exchange resin column. The HCl solution was evaporated almost to dryness, diluted to 1 M in HCl . Silver carrier was added and the AgCl precipitate centrifuged. Copper carrier was added, H_2S passed, and the acid insoluble sulfides centrifuged. After evaporating the solution almost to dryness, HCl was destroyed with HNO_3 , the solution diluted to 1 M in HNO_3 , an excess of Na_2BiO_3 added, and the solution boiled to oxidize Mn^{+3} to MnO_4^- . Iron carrier was added, the solution made basic with NaOH and the basic insoluble hydroxides centrifuged. After making the solution 1 M in HNO_3 , MnO_4^- was reduced with oxalic acid, excess BrO_3^- added, the solution boiled until MnO_2 coagulated, and MnO_2 centrifuged. The anion exchange column, AgCl , CuS scavenges, the bismuthate oxidation, the $\text{Fe}(\text{OH})_3$ scavenge, the oxalate reduction, and the MnO_2 precipitation were repeated. The MnO_2 was dissolved in dilute HNO_3 plus H_2O_2 , diluted further, MnO_2 reprecipitated, centrifuged, washed twice with water, twice with acetone, ignited in a porcelain crucible at 900° F and weighed as Mn_3O_4 .

Iron:--Iron and cerium carriers were added to the Ta target solution, the rare earth fluorides centrifuged, the solution made 18 N in H_2SO_4 , Ta extracted with di-isopropyl ketone, and the aqueous layer evaporated almost to dryness. The residue was dissolved in H_2O , made basic with NH_4OH , the $Fe(OH)_3$ precipitate centrifuged and washed with dilute ammonia. The $Fe(OH)_3$ was dissolved in concentrated HCl , diluted to 7.5 N in HCl , the Fe extracted with isopropyl ether, and the ether layer washed with 7.5 N HCl . After Fe had been back extracted into buffered acetic acid-acetate solution, Mo, Ga, Sb, Sn, and Ge carriers were added; the solution was made basic with $NaOH$, centrifuged, and the $Fe(OH)_3$ washed with dilute $NaOH$. The $Fe(OH)_3$ was dissolved in 3 N HCl , Mo, Ga, Sb, As, Ce carriers were added, H_2S passed in, and the acid insoluble sulfides centrifuged. The solution was made basic with NH_4OH , centrifuged, and the Fe_2S_3 precipitate washed with dilute NH_4OH . The Fe_2S_3 was dissolved in concentrated HNO_3 , scavenged with WO_3 , made basic with $NaOH$, and the $Fe(OH)_3$ centrifuged. The ether extraction and $Fe(OH)_3$ precipitation were repeated twice with the final $Fe(OH)_3$ precipitate being washed twice with dilute NH_4OH , ignited in a platinum crucible at $900^\circ F$ and weighed as Fe_2O_3 .

Cobalt:--Cobalt and cerium carriers were added to the Ta target solution, the rare earth fluorides centrifuged, the solution made 18 N in H_2SO_4 , Ta extracted with di-isopropyl ketone, and the aqueous layer evaporated almost to dryness. The residue was dissolved in water, Fe carried added, made basic with NH_4OH , and the $Fe(OH)_3$ precipitate centrifuged. Hydrogen sulfide was passed in, the CoS was centrifuged

and washed with dilute NH_4OH . The CoS was dissolved in concentrated HCl , boiled to expel H_2S , concentrated HCl added, and the solution passed through a 2 mm x 5 cm Dowex A-2 column, after which the resin was washed with concentrated HCl . Cobalt was eluted with 3 N HCl , the eluant diluted to 1 N in HCl , Ag carrier added and the AgCl precipitate centrifuged. Iron was added, made basic with NH_4OH , and the $\text{Fe}(\text{OH})_3$ centrifuged. Hydrogen sulfide was passed in, the CoS precipitate centrifuged and washed with dilute NH_4OH . Cobalt sulfide was dissolved in concentrated HCl , boiled to evaporate the H_2S , diluted to 0.1 N in HCl , a large excess of KCNS added, and Co extracted with a 1:1 mixture of amyl alcohol:ether. Cobalt was back extracted into 6 N NH_4OH , H_2S was passed in, and the CoS centrifuged. The anion exchange column separation was repeated. The 3 N HCl solution was evaporated just to dryness, Co dissolved in water, buffered with acetic acid-acetate, a large excess of fresh concentrated KNO_2 solution added, and the solution centrifuged. The precipitate was washed twice with water, twice with acetone, dried at 110°C for twenty minutes and weighed as $\text{K}_3\text{Co}(\text{NO}_2)_6 \cdot 6\text{H}_2\text{O}$.

Nickel:--Nickel and cerium carriers were added to the Ta target solution, the rare earth fluorides centrifuged, the solution made 18 N in H_2SO_4 , Ta extracted with di-isopropyl ketone, and the aqueous layer evaporated almost to dryness. The residue was dissolved in H_2O , Fe carrier added, the solution made basic with NH_4OH , and $\text{Fe}(\text{OH})_3$ centrifuged. Dimethylglyoxime was added and the nickel dimethylglyoxime precipitate was filtered and washed with dilute NH_4OH . The precipitate was dissolved in concentrated HNO_3 , boiled to destroy dimethylglyoxime,

HNO_3 destroyed with HCl , diluted, Ag carrier added, and AgCl centrifuged; Cu carrier was added, H_2S passed in, and CuS centrifuged. After H_2S had been expelled by boiling, Fe carrier was added, the solution made basic with NH_4OH , and $\text{Fe}(\text{OH})_3$ centrifuged. Palladium carrier was added, the solution adjusted to pH 3 with HCl , dimethylglyoxime added, and the palladium dimethylglyoxime filtered, after which the solution was made basic with NH_4OH and the nickel dimethylglyoxime filtered. The AgCl , CuS , $\text{Fe}(\text{OH})_3$ scavenges and the nickel dimethylglyoxime precipitations were repeated. The final nickel dimethylglyoxime was washed twice with water, twice with ethanol, dried at 110°C and weighed as nickel dimethylglyoxime.

Copper:--Copper and cerium carriers were added to the Ta target solution, the rare earth fluorides centrifuged, saturated KF solution added, and the K_2TaF_7 precipitate centrifuged. Iron carrier was added, the solution made basic with NH_4OH , and the $\text{Fe}(\text{OH})_3$ precipitate centrifuged. The solution was adjusted to pH 1 with HCl , H_2S was bubbled through, and the CuS centrifuged and washed with 0.4 M HCl . The CuS was dissolved in HNO_3 , boiled to destroy sulfide, Fe, Ba carriers added, the solution made basic with NH_4OH , $(\text{NH}_4)_2\text{CO}_3$ added, and the $\text{Fe}(\text{OH})_3$ and BaCO_3 precipitates centrifuged. The solution was made 0.1 N with HCl , SO_2 passed in to reduce copper, KCNS added, and CuCNS centrifuged. The precipitate was dissolved in HNO_3 , neutralized with NH_4OH , KCN , Cd, As carriers added, H_2S passed in, and the sulfide precipitate centrifuged. The solution was acidified, boiled to remove the HCN , made 3 N in HCl , H_2S passed in, and the CuS centrifuged. The precipitate was dissolved in HNO_3 , scavenged with AgCl , $(\text{Fe}(\text{OH})_3)$, and BaCO_3 , and the CuCNS precipitation repeated. The CuCNS was dissolved

in HNO_3 and the CuCNS precipitation repeated. The final precipitate was washed twice with water, twice with ethanol, dried at 110°C and weighed as CuCNS .

Gallium: -- Gallium and lanthanum carriers were added to the Ta target solution, the rare earth fluorides centrifuged, concentrated KF solution added, the K_2TaF_7 precipitate centrifuged, washed with water, and the washings combined with the original solution. The supernatant was made 7 N in HCl ; gallium was extracted with di-isopropyl ketone and back extracted with water. The aqueous layer was adjusted to the yellow brom cresol purple end point with NaOH , $\text{pH } 5.5$ acetic acid-acetate buffer was added, and the $\text{Ga}(\text{OH})_3$ precipitate centrifuged. The hydroxide was dissolved in dilute HCl , Cu added, H_2S passed in, and the CuS precipitate centrifuged. After H_2S had been removed by boiling, the $\text{Ga}(\text{OH})_3$ precipitation was repeated. The precipitate was dissolved in 6 N HCl , Ga extracted with isopropyl ether, back extracted into water, and the $\text{Ga}(\text{OH})_3$ precipitation repeated. The hydroxide was dissolved in dilute acid, oxine-acetic acid solution added, digested at 60°C , centrifuged, and the precipitate washed twice with water, twice with ethanol, dried at 110°C and weighed as gallium-8 hydroxyquinolate.

Arsenic: -- Arsenic and cerium carriers were added to the Ta target solution, the rare earth fluorides centrifuged, formic acid added, and the solution heated until HNO_3 had been reduced. The solution was made 6 N in HCl , H_2S passed in, the As_2S_3 precipitate centrifuged, and washed with 6 N HCl saturated with H_2S . The As_2S_3 was dissolved in concentrated NH_4OH , Te , Sb , Sn , Ge carriers were added, and any

precipitate centrifuged. The solution was made 6 N in HCl, H₂S passed in, and the As₂S₃ precipitate centrifuged. The As₂S₃ was dissolved in concentrated NH₄OH, transferred to a glass still; Ge carrier, concentrated HCl, and KClO₃ crystals were added and the GeCl₄ distilled. To the residue saturated CuCl in concentrated HCl was added, the AsCl₃ was distilled in a stream of HCl and the distillate was collected in ice cold concentrated HCl. Hydrogen sulfide was passed into the distillate, the As₂S₃ precipitate was centrifuged and washed with 6 N HCl. The GeCl₄ and AsCl₃ distillations and the As₂S₃ precipitation were repeated. The final As₂S₃ precipitate was washed twice with 6 N HCl, twice with water, twice with ethanol, dried at 110° C and weighed as As₂S₃.

Bromine:--The Ta target was dissolved in the presence of Br carrier in a distillation flask. When the target was dissolved additional Br carrier was added and the solution was heated in a stream of air to complete the distillation, the distillate being trapped in 0.5 M Na₂SO₃ solution. The distillate was made 1 M in HNO₃, heated to destroy SO₃⁼, I⁻ carrier and 0.1 M NaNO₂ solution added, and I₂ extracted with CCl₄. Potassium permanganate solution was added and Br₂ was extracted with CCl₄ and back extracted into water containing enough SO₃⁼ to reduce the Br₂. The I₂ and Br₂ extractions were repeated twice. The last SO₃⁼ solution of Br was made 1 M in HNO₃, heated to destroy SO₃⁼, Ag carrier added, the AgBr centrifuged. The precipitate was washed twice with 1 M HNO₃ twice with water, twice with ethanol, dried at 110° C and weighed as AgBr.

Rubidium:--Rubidium carrier was added to the Ta target solution. The potassium chemistry up to the point where the K, Rb, and Cs perchlorates are placed on the Duolite C-3 cation exchange resin column was repeated. The activity was eluted with 0.3 M HCl solution. Potassium came off quickly and could be discarded; rubidium came off next, and cesium trailed far behind. The rubidium fraction was evaporated almost to dryness, concentrated HClO_4 added, evaporated almost to dryness, cooled, and the RbClO_4 precipitate was washed four times with ice cold ethyl acetate, dried under a heat lamp and weighed as RbClO_4 .

Strontium:--Strontium and cerium carriers were added to the Ta target solution, the rare earth fluorides centrifuged, H_2SO_4 added, and the SrSO_4 precipitate was centrifuged and washed with dilute H_2SO_4 . The SrSO_4 precipitate was metathesized twice with an Na_2CO_3 -NaOH solution, centrifuged, and washed with dilute Na_2CO_3 solution. The SrCO_3 precipitate was dissolved in a minimum volume of dilute HNO_3 , ice cold red fuming HNO_3 was added, and the $\text{Sr}(\text{NO}_3)_2$ precipitate was centrifuged. The precipitate was dissolved in water, Fe carrier added, the solution made basic with NH_3 gas (CO_2 free) and the $\text{Fe}(\text{OH})_3$ scavenge centrifuged. Ammonium carbonate was added the the SrCO_3 precipitate centrifuged. The $\text{Sr}(\text{NO}_3)_2$ precipitation, the $\text{Fe}(\text{OH})_3$ scavenge, and the SrCO_3 precipitation were repeated. The SrCO_3 was dissolved in dilute HNO_3 , Ba carrier was added, the solution buffered to pH 5 with acetate, Na_2CrO_4 solution added, and the BaCrO_4 centrifuged. The BaCrO_4 precipitation was repeated twice. The solution was made basic with NH_4OH , $(\text{NH}_4)_2\text{CO}_3$ solution added, and the SrCO_3 precipitate centrifuged. The precipitate was dissolved in dilute HNO_3 , the SrCO_3 precipitation

repeated, and the SrCO_3 washed four times with dilute NH_4OH , dried at 110°C , and weighed as SrCO_3 .

Zirconium:--Zirconium, Hf, and Ce carriers were added to the Ta target solution, the rare earth fluorides centrifuged, the solution cooled in an ice bath, and ice cold saturated $\text{Ba}(\text{NO}_3)_2$ solution was added dropwise with constant stirring. The BaZrF_6 precipitate was centrifuged and washed with ice cold water. The precipitate was dissolved in ice cold saturated H_3BO_3 plus concentrated HNO_3 , the solution made basic with NH_4OH , and the $\text{Zr}(\text{OH})_4$ precipitate was centrifuged and washed with dilute NH_4OH . The hydroxide was dissolved in 1 M HNO_3 , Zr extracted into 0.4 M thenoyltrifluoroacetone (TIA)-benzene solution, and back extracted into 5 percent NH_4HF_2 solution. Saturated H_3BO_3 was added to the aqueous layer, the solution made basic with NH_4OH , and the $\text{Zr}(\text{OH})_4$ centrifuged. The hydroxide was dissolved in 1 M HF and the BaZrF_6 and the $\text{Zr}(\text{OH})_4$ precipitations repeated. At this point Zr should have been purified from everything except Hf. The hydroxide was dissolved in 3 N HClO_4 , heated to break up colloids, and passed through a 5 mm x 20 cm Dowex-50 cation exchange resin column (Zr and Hf were both adsorbed). The column was washed with water, then 50 ml. of 1.00 N H_2SO_4 was passed through, Zr being removed. Hafnium remained on the column. The eluant was made basic with NH_4OH and the $\text{Zr}(\text{OH})_4$ precipitate centrifuged. The Zr-Hf ion exchange column separation was repeated three times (four column separations in all). The final hydroxide precipitate was dissolved in 3 N HNO_3 , H_3PO_4 added, centrifuged, the precipitate washed twice with 3 N HNO_3 , twice with acetone, ignited at 900°F , and weighed as ZrP_2O_7 .

Molybdenum:--Molybdenum, tungsten and cerium carriers were added to the Ta target solution, the rare earth fluorides centrifuged, saturated KF solution added, the K_2TaF_7 precipitate centrifuged, washed with water, and the washings returned to the original solution. Iron carrier was added, the solution made basic with NH_4OH , and the $Fe(OH)_3$ centrifuged. Copper carrier was added, H_2S passed in, and the CuS scavenge centrifuged. The solution was adjusted to pH 3, heated, H_2S passed in, the MoS_3 precipitate centrifuged, and washed with pH 3 solution saturated with H_2S . The sulfide was destroyed with concentrated HNO_3 , diluted, adjusted to the red methyl orange end point with NH_4OH , buffered with acetate, $AgNO_3$ added, and the Ag_2MoO_4 precipitate centrifuged. The precipitate was dissolved in concentrated NH_4OH and the $Fe(OH)_3$ and CuS scavenges and the MoS_3 and Ag_2MoO_4 precipitations were repeated. The final Ag_2MoO_4 precipitate was washed twice with water, twice with ethanol, dried at $110^\circ C$, and weighed as Ag_2MoO_4 .

Ruthenium:--Ruthenium and cerium carriers were added to the Ta target solution, the rare earth fluorides centrifuged, the solution made $6 N$ in HCl , Ta extracted with di-isopropyl ketone, and the aqueous layer evaporated almost to dryness. Concentrated $HClO_4$ was added and RuO_4 distilled in an air stream, the distillate being collected in ice cold $6 N NaOH$. Ethanol was added to the distillate, boiled, centrifuged, and the ruthenium hydroxide washed with dilute $NaOH$. The precipitate was dissolved in concentrated HCl , evaporated almost to dryness, and the distillation and hydroxide precipitations repeated. The hydroxide was dissolved in $1 N HCl$ and ruthenium

reduced to the metal with magnesium chips, excess Mg being destroyed with HCl. The metal was centrifuged, washed twice with water, twice with ethanol, dried at 110° C and weighed as Ru.

Rhodium:--Rhodium, palladium and cerium carriers were added to the Ta target solution, the rare earth fluorides centrifuged, the solution was made ice cold, 4 percent NaI solution added, and the PdI_2 precipitate centrifuged. Twenty percent NaI solution was added, the solution was boiled for 15 minutes, and the RhI_3 precipitate centrifuged. The RhI_3 was dissolved in concentrated H_2SO_4 , fumed almost to dryness, cooled, diluted to 0.5 N, the solution passed through a 2 mm x 5 cm Dowex-50 cation exchange resin column, and the resin washed with H_2O . The sulfate eluant solution was adjusted to pH 5, a large excess of KNO_2 was added, and after boiling for 5 minutes, the $\text{K}_3\text{Rh}(\text{NO}_2)_6$ precipitate was centrifuged and washed with water. The rhodinitrite was dissolved in concentrated HClO_4 and evaporated almost to dryness. The HClO_4 fuming was repeated four times, after which the residue was dissolved in water and passed through a 2 mm x 5 cm Dowex-50 column (Rh was adsorbed), and the resin washed with water. Rhodium was eluted with hot 2 N HCl, the eluant diluted to 1 N HCl and Rh reduced to the metal with Mg chips, excess Mg being destroyed with HCl. The metal was washed twice with water, twice with ethanol, dried at 110° C and weighed as Rh.

Palladium:--Palladium and cerium carriers were added to the Ta target solution, the rare earth fluorides centrifuged, the solution made 18 N in H_2SO_4 , Ta extracted with di-isopropyl ketone, and the aqueous layer evaporated almost to dryness. The residue was

dissolved in water, Fe carrier was added, the solution made basic with NH_4OH , and the $\text{Fe}(\text{OH})_3$ centrifuged. The solution was adjusted to pH 2 with HCl, Ag carrier was added, and the AgCl centrifuged. Nickel carrier and dimethylglyoxime were added and the palladium dimethylglyoxime filtered and washed with 0.1 N HCl. The precipitate was dissolved in concentrated HNO_3 and boiled to destroy the dimethylglyoxime. The $\text{Fe}(\text{OH})_3$ and AgCl scavenges and the palladium dimethylglyoxime precipitation were repeated twice. The final palladium dimethylglyoxime precipitate was washed twice with water, twice with ethanol, dried at 110°C , and weighed as palladium dimethylglyoxime.

Silver:--The target was dissolved in the presence of Ag carrier, HCl added, and the AgCl precipitate centrifuged and washed with dilute HCl. The AgCl was dissolved in 6 N NH_4OH , Fe carrier was added, and the $\text{Fe}(\text{OH})_3$ centrifuged. The $\text{Fe}(\text{OH})_3$ scavenge was repeated. Hydrogen sulfide was passed in, and the Ag_2S centrifuged and washed with dilute NH_4OH . The Ag_2S was dissolved in concentrated NH_4OH , boiled to destroy the sulfide, diluted, HCl added, and the AgCl centrifuged. The $\text{Fe}(\text{OH})_3$ scavenge and the Ag_2S and AgCl precipitations were repeated twice. The final AgCl precipitate was washed twice with 1 M HNO_3 , twice with ethanol, dried at 110°C and weighed as AgCl.

Cadmium:--Cadmium and cerium carriers were added to the Ta target solution, the rare earth fluorides centrifuged, the solution made 18 N in H_2SO_4 , Ta extracted with di-isopropyl ketone, and the aqueous layer evaporated almost to dryness. The residue was dissolved in water, Fe carrier was added, the solution made basic with NH_4OH , and the $\text{Fe}(\text{OH})_3$

centrifuged. Hydrogen sulfide was passed in, the CdS centrifuged, and washed with dilute NH_4OH . The precipitate was dissolved in 2 N HCl , Cu carrier was added, H_2S passed in and the CuS precipitate centrifuged. The solution was boiled to expel excess H_2S , Zn carrier was added, and the solution was passed through a 2 mm x 5 cm Dowex A-2 anion exchange column (Cd was adsorbed), and the resin washed with 0.1 M HCl . Cadmium was eluted with 1.5 N H_2SO_4 , H_2S was passed through the eluent, centrifuged, and CdS washed with 1.5 N H_2SO_4 . The anion exchange column separation (without Zn holdback carrier) was repeated. The final H_2SO_4 eluant was adjusted to pH 4 with NH_4OH , boiled, $(\text{NH}_4)_2\text{HPO}_4$ solution added, and the precipitate centrifuged, washed twice with water, twice with ethanol, dried at 110°C , and weighed as $\text{Cd}(\text{NH}_4)\text{PO}_4 \cdot \text{H}_2\text{O}$.

Indium:--Indium and cerium carriers were added to the Ta target solution, the rare earth fluorides centrifuged, the solution made 18 N in H_2SO_4 , Ta extracted with di-isopropyl ketone, and the aqueous layer evaporated almost to dryness. The residue was dissolved in H_2O , made just basic with NH_4OH , and the $\text{In}(\text{OH})_3$ centrifuged. The precipitate was dissolved in HCl , Sn, Sb, Te, Se, Ga, W, and Hf carriers were added, the solution made basic with NaOH , and $\text{In}(\text{OH})_3$ centrifuged. The hydroxide was dissolved in 7.5 N HCl . Indium was extracted with di-isopropyl ketone and back extracted into water. Tin, Sb, As, Cu carriers were added, H_2S passed in and the acid sulfides centrifuged. The solution was boiled to expel H_2S , made basic with NaOH , and the $\text{In}(\text{OH})_3$ centrifuged. The precipitate was dissolved in 7.5 N HCl , Fe, Ga carriers were added and extracted with isopropyl ether. Indium

was extracted with di-isopropyl ketone and back extracted into water. The aqueous layer was made basic with NH_4OH , and $\text{In}(\text{OH})_3$ centrifuged. The hydroxide was dissolved in very dilute HCl , and the solution was passed through a 2 mm x 5 cm Dowex-50 cation exchange column. The resin was washed with water and In eluted with 3 N HCl . The eluant was made basic with NH_4OH , the $\text{In}(\text{OH})_3$ centrifuged, washed four times with dilute NH_4OH , ignited in a platinum crucible at 800°C , and weighed as yellow In_2O_3 .

Tellurium:--Tellurium, selenium and cerium carriers were added to the Ta target solution, the rare earth fluorides were centrifuged, H_2S was passed in, the TeS_2 centrifuged and washed with 6 N HCl . The TeS_2 was dissolved in concentrated HNO_3 , evaporated almost to dryness, the residue dissolved in 6 N NaOH , and scavenged with $\text{Fe}(\text{OH})_3$. The supernatant was made 3 N in HCl , SO_2 was passed in, the Te centrifuged, and washed with water. The precipitate was dissolved in concentrated HNO_3 , evaporated to dryness, dissolved in concentrated HCl , SO_2 passed in, and the Se centrifuged. The solution was diluted to 3 N in HCl , SO_2 passed in, and Te centrifuged. The ferric hydroxide scavenge and the SO_2 reduction was repeated twice. The final Te precipitate was washed twice with water, twice with ethanol, dried at 110°C and weighed as Te.

Cesium:--Cesium carrier was added to the Ta target solution. The potassium chemistry up to the point where K, Rb, and Cs perchlorates are placed on the Duolite C-3 cation exchange resin column was followed. The activity was eluted with 0.3 N HCl until all of the potassium and rubidium had been removed, and then Cs was eluted with

6 N HCl. The cesium fraction was evaporated almost to dryness, concentrated HClO_4 was added and evaporated almost to dryness, cooled, and the CsClO_4 precipitate washed four times with ice cold ethyl acetate, dried under a heat lamp and weighed as CsClO_4 .

Barium:--Barium and Ce carriers were added to the Ta target solution, the rare earth fluorides centrifuged, H_2SO_4 was added, the BaSO_4 centrifuged, and washed with dilute H_2SO_4 . The BaSO_4 was metathesized twice with $\text{NaOH-Na}_2\text{CO}_3$. Barium carbonate was dissolved in dilute HNO_3 , ice cold red fuming HNO_3 was added, and the $\text{Ba}(\text{NO}_3)_2$ centrifuged. The precipitate was dissolved in water, Fe carrier was added, the solution made basic with NH_3 gas (CO_2 free), and $\text{Fe}(\text{OH})_3$ centrifuged. Ammonium carbonate was added and BaCO_3 centrifuged. The $\text{Ba}(\text{NO}_3)_2$ precipitation, the ferric hydroxide scavenge and the BaCO_3 precipitation were repeated once. Barium carbonate was dissolved in water, Sr carrier was added, the solution was buffered at pH 5 with acetate, Na_2CrO_4 solution added, and the BaCrO_4 centrifuged and washed with dilute acetate buffer. The BaCrO_4 was dissolved in a minimum volume of 6 N HCl, ice cold 5:1 solution of concentrated HCl:ether was added, the BaCl_2 centrifuged, and washed with ether reagent. The precipitate was dissolved in water, the BaCrO_4 precipitation was repeated, and the final precipitate was washed twice with water, twice with ethanol, dried at 110°C and weighed as BaCrO_4 .

Cerium:--The Ta target was dissolved in the presence of Ce and La carriers. The rare earth fluorides were centrifuged, washed with water, and dissolved in saturated H_3BO_3 plus concentrated HNO_3 solution. The solution was made basic with NH_4OH and the rare earth

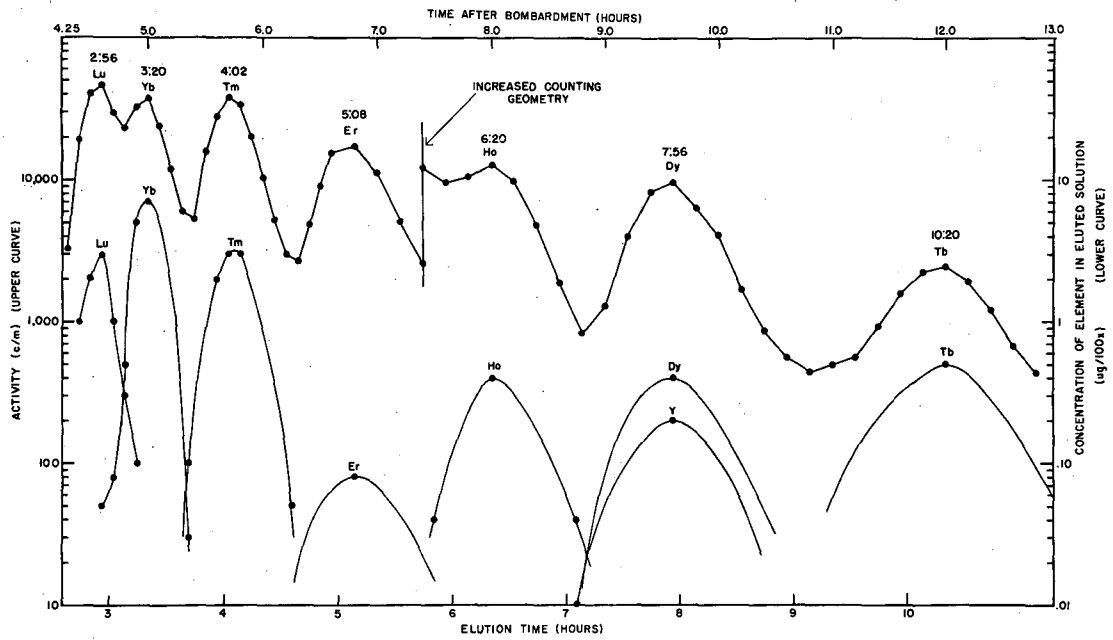
hydroxides centrifuged and washed with dilute NH_4OH . The precipitate was dissolved in HCl and the fluoride and hydroxide precipitations repeated. The hydroxide was dissolved in 6 N HNO_3 , solid $(\text{NH}_4)_2\text{S}_2\text{O}_8$ and AgNO_3 were added, and Ce was extracted into 30 percent tributyl phosphate in CCl_4 . Cerium was back extracted into a 1 N HCl solution containing Na_2SO_3 . The aqueous layer was made basic with NH_4OH , $\text{Ce}(\text{OH})_3$ centrifuged and washed with dilute NH_4OH . The precipitate was dissolved in HCl , Zr, Ta, W, and Hf carriers were added, and the fluoride and hydroxide precipitations, the TBP extraction, and the hydroxide precipitation were repeated. The final hydroxide was dissolved in dilute HCl , saturated oxalic acid was added, and the precipitate was washed twice with water, twice with ethanol, dried by evacuation in a desiccating flask and weighed as $\text{Ce}_2(\text{C}_2\text{O}_4)_3 \cdot 10\text{H}_2\text{O}$.

Rare Earths:--The Ta target was dissolved in the presence of carriers of all of the rare earths that were to be separated and the rare earth fluorides were centrifuged and washed with water. The fluorides were dissolved in saturated H_3BO_3 and concentrated HNO_3 , the solution made basic with NH_4OH , and the rare earth hydroxides were centrifuged and washed with dilute NH_4OH . The precipitate was dissolved in HCl and the rare earth fluoride and hydroxide precipitations repeated. The final hydroxide precipitate was dissolved in a minimum of HCl , diluted and transferred to a Dowex-50 cation exchange resin column.

Data existing at the time the rare earth separations were begun indicated that use of citrate as an eluting agent would probably not give satisfactory separations of the heavy rare earths in the short

times required. Therefore, a technique was developed in which lactic acid was used as the eluting agent. Figure 2 shows one of the earliest elution curves obtained by this method. On this particular run the rare earths were placed in a thin layer on top of a resin column 14 mm in diameter and 43 cm long made up of 4 percent cross linked Dowex-50 resin of 250-400 mesh size. The entire column was surrounded by a jacket through which trichloroethylene vapors were kept circulating. Lactic acid, 0.43 M, adjusted to a pH of 3.40 with concentrated NH_4OH , was passed through the resin bed at a flow rate of $0.35 \text{ ml/cm}^2/\text{min}$ and samples were collected at three minute intervals. The elution curve of Figure 2 was obtained by evaporating aliquots from the sample tubes on thin aluminum plates, counting the activity on the plates in a Geiger counter and plotting activity versus time of the sample. It is well known that elution rates will vary sharply as a function of the pH of the eluting agent. On most of the tantalum bombardments (where separation of the heavy rare earths was desired) the pH was kept at 3.40. On a number of separations, however, the pH was changed. Figure 3 shows how the eluting times varied as a function of pH. Here the free column volumes of eluting agent required to reach the elution peak for each element are plotted against pH.

When bombardments were run in which cross sections were to be obtained, approximately 5 mg of carrier of the desired element was added to the target solution. No weighable amounts of carriers of the two adjacent rare earths were added. By this method errors in the chemical yield figures due to cross contamination of the peaks were minimized.



MU 5640

Figure 2. Rare earth elution curve
using lactic acid.

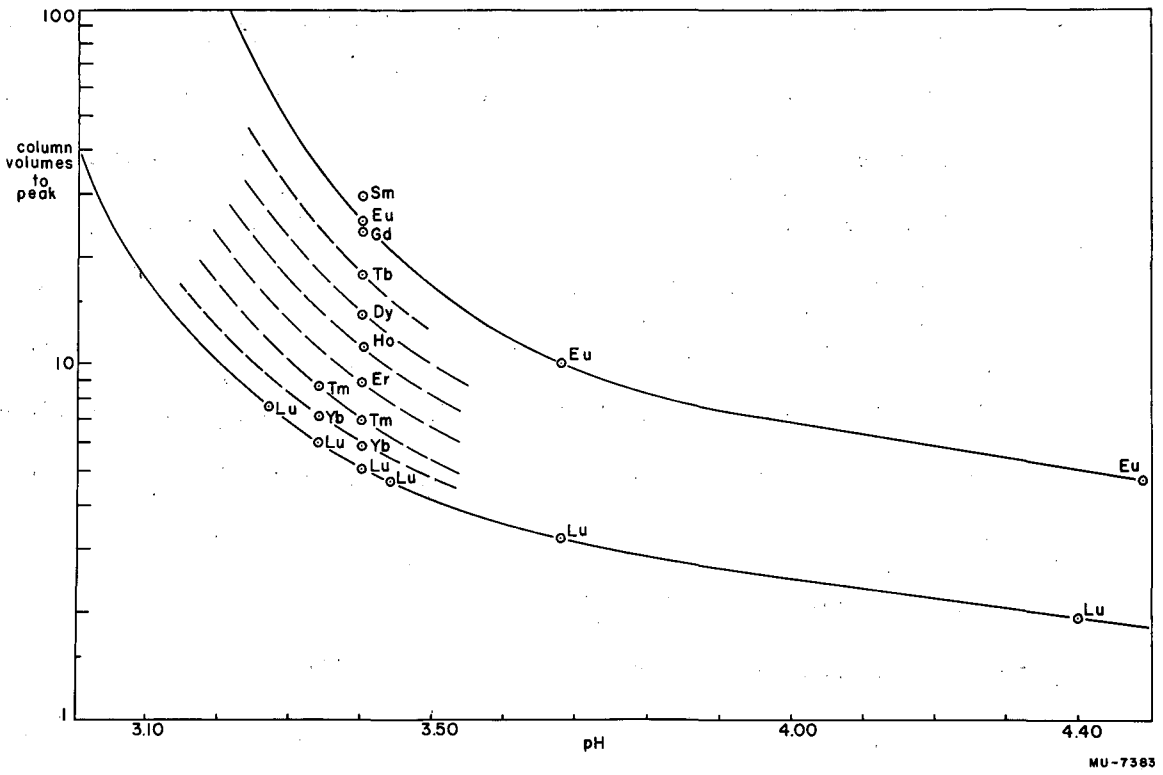


Figure 3. Rare earth eluting time as a function of pH.

When the column separation had been completed, individual elemental fractions were evaporated to dryness, the residual lactate destroyed with fuming H_2SO_4 and 30 percent H_2O_2 , and the residue dissolved in water. The rare earth hydroxides were precipitated and dissolved in dilute HCl. The rare earth oxalates were precipitated, washed twice with water, twice with ethanol, ignited at $1600^\circ F$, and weighed as the rare earth oxides.

Hafnium:--Hafnium and cerium carriers were added to the Ta target solution, the rare earth fluorides were centrifuged, the solution was cooled and ice cold saturated $Ba(NO_3)_2$ was added dropwise. The $BaHfF_6$ precipitate was washed with ice cold water. The precipitate was dissolved in ice cold saturated H_3BO_3 and concentrated HNO_3 , the solution made basic with NH_4OH , centrifuged, and the precipitate washed with water. The $Hf(OH)_4$ was dissolved in 1 M HF, and the rare earth fluoride scavenge and the $BaHfF_6$ and $Hf(OH)_4$ precipitations were repeated. The $Hf(OH)_4$ was dissolved in 3 N $HClO_4$, Hf was extracted with 0.4 M thenoyltrifluoroacetone (TTA) in benzene and back extracted into a 5 percent solution of NH_4HF_2 . Boric acid was added to complex the fluoride, the solution made basic with NH_4OH , centrifuged, and the $Hf(OH)_4$ washed with dilute NH_4OH . The hydroxide was dissolved in 3 N H_2SO_4 , H_3PO_4 added, centrifuged, and the precipitate washed twice with 3 N H_2SO_4 , twice with water, twice with acetone, ignited at $1600^\circ F$, and weighed as HfP_2O_7 .

Tantalum:--The target was dissolved in HF-HNO₃ with Ce carrier added. The rare earth fluorides were centrifuged, Hf and W carriers and saturated $Ba(NO_3)_2$ solution were added and the $BaHfF_6$ precipitate

centrifuged. The solution was made 18 N in H_2SO_4 , Ta was extracted with di-isopropyl ketone, and the DIPK layer washed with 18 N H_2SO_4 -2N HF solution. Tantalum was back extracted with dilute H_3BO_3 . Tungsten carrier was added, the solution made basic with NH_4OH , and the hydroxide centrifuged and washed with dilute NH_4OH . Ice cold red fuming HNO_3 was added, the tantalic acid was centrifuged and washed with fuming HNO_3 . The precipitate was dissolved in 2 N HF and the CeF_3 , $BaHF_6$ scavenges, the Ta extraction, and the hydroxide and acid precipitations were repeated. The final acid precipitate was washed twice with fuming HNO_3 , twice with water, twice with acetone, ignited at $1600^\circ F$ in a porcelain crucible and weighed as Ta_2O_5 .

Tungsten:--The Ta target was dissolved in the presence of W and Ce carrier. The rare earth fluorides were centrifuged, concentrated KF solution was added, the K_2TaF_7 precipitate centrifuged, and the solution evaporated to dryness in a platinum crucible. The residue was dissolved in concentrated NH_4OH , diluted to 3 N and scavenged with $Ce(OH)_3$. The solution was adjusted to pH 6-7 with HCl, $CoCl_2$ solution was added, and $CoWO_4$ centrifuged and washed with water. The $CoWO_4$ precipitate was digested in 6 N HCl until the WO_3 precipitate coagulated and turned yellow when the precipitate was centrifuged. The WO_3 was dissolved in NH_4OH , the solution was adjusted to pH 6 with HCl, Hg_2Cl_2 , and NH_4SCN were added, the solution was made 2 N in HCl, and the green tungsten thiocyanate complex was extracted with ethyl acetate. The organic layer was washed with 2 N HCl and W was back extracted into basic oxalate solution. The aqueous layer was

acidified with H_2SO_4 , oxalate was destroyed with bromate, the solution was heated until the yellow WO_3 coagulated and the WO_3 was then centrifuged. The WO_3 was dissolved in NH_4OH and the $CoWO_4$ and WO_3 precipitations were repeated. The final precipitate was washed twice with 2 N HCl , twice with water, twice with acetone, ignited and weighed as WO_3 .

III. RADIOACTIVE NUCLIDES OBSERVED

A. Resolution of Decay Curves

Examination of previous spallation-fission data indicated that most of the individual element fractions from these tantalum bombardments would probably consist of more than one active nuclide. Some of the elements when purified should have only one or two activities which could easily be separated and identified. In others, notably tungsten and hafnium, it was conceivable that there would be five active nuclides in the fraction immediately after purification and that four daughter activities could "grow in" during the decay of the parents, giving a nine component gross decay curve. It was necessary that these multiple component decay curves be resolved into their individual activities since the activity of a nuclide must be used in calculating formation cross sections.

In principle the total activity of a given sample may be expressed as a sum of exponential terms and should be resolvable, one component at a time. In practice this is feasible only in relatively simple mixtures where the half-lives of the activities involved differ by more than a factor of two. For a two component decay curve in which

the half-lives are comparable, the activities may be resolved analytically by a "Biller Plot".¹⁴ In this technique the total activity may be expressed as:

$$\Sigma A = A_1^{\circ} e^{-\lambda_1 t} + A_2^{\circ} e^{-\lambda_2 t}$$

where A_1° and A_2° are the initial activities and λ_1 , λ_2 are the decay constants of the two components. Multiplying by $e^{+\lambda_2 t}$ gives:

$$e^{\lambda_2 t} \Sigma A = A_1^{\circ} e^{(\lambda_2 - \lambda_1)t} + A_2^{\circ}$$

Plotting $e^{\lambda_2 t} \Sigma A$ versus $e^{(\lambda_2 - \lambda_1)t}$ gives a straight line whose slope is A_1° and whose intercept on the $e^{\lambda_2 t} \Sigma A$ axis is A_2° .

When the total activity consists of three or more components, it is often possible to separate them by counting through absorbers. Thus the components having the least penetrating radiations may be blocked off and the decay curves of the remaining components may be more easily resolved. Caution must be taken with this technique, however, since it is very seldom that all of the radiations from one component may be absorbed completely and still allow enough of the radiation from the remaining components to pass. Usually only 90 or 95 percent of a weak component is blocked out and this must be taken into account in analyzing the resulting decay curves.

When the total activity consists of many components it is often most practical to get the activity of individual nuclides by "milking" their daughter activities chemically and counting them separately. The activity of the parent at the end of bombardment is then related to the activity of the daughter at the time of chemical separation by:

$$A_1^0 = \frac{1}{C_2} \frac{\lambda_1 - \lambda_2}{\lambda_2} A_2^0(t_{\text{sep}}) e^{\lambda_1 t_{\text{sep}}}$$

where A_1^0 , A_2^0 are the activities of parent and daughter, λ_1 and λ_2 their decay constants, C_2 the counting efficiency of the daughter, and t_{sep} the time from the end of the bombardment to the time of chemical separation. Very often when the total activity cannot be resolved by any of the foregoing methods, it is possible to separate activities by following the decays of the sample on a scintillation counter. If the decay schemes are known, it is usually possible to identify individual gamma rays and follow their decay in the midst of all other gamma radiation.

After each element fraction had been separated and purified, decay of the gross activity was followed by that means which would give the most accurate resolution for the components involved.

Wherever possible, samples were counted on a Geiger-Müller counter. The counting unit itself was an end window, chlorine-argon filled Amperex type 100C tube mounted in such a way that samples could be placed in any of five fixed counting positions which ranged from 0.46 to 6.81 cm. from the end of the tube. This whole assembly was housed inside a 2 inch thick lead castle to reduce background radiation and the lead was lined with aluminum to minimize scattering of radiation from the inner walls of the castle. When used in conjunction with a scale of 256 scaling unit, this counter could handle activities of 80 to 100,000 counts per minute without difficulty. At these high counting rates, however, the time between entry of successive beta particles into the sensitive volume of the

Geiger-Müller tube becomes small compared to the resolving time of the counting circuit. In order to get the actual number of particles entering the counter, it is then necessary to correct the observed counting rate for these coincident events. There are a number of ways of obtaining these coincidence correction factors. The simplest, and the one used in these experiments, involves counting a pure sample which has a known half-life (61 hour Y^{90} in this case) while it decays from an initial counting rate of over 100,000 counts per minute (where the coincidence correction is large) to a rate of less than 1,000 counts per minute (where coincidences are negligible). From the final counting rate and the known decay constant the actual rate of each of the initial counts may be calculated. The coincidence correction may then be obtained by difference.

For samples in which the gamma radiation was of interest the gamma spectra were obtained on a 50-channel gamma pulse height analyzer. The counting unit in this instrument was a 1 inch thick NaI-Tl activated scintillation crystal used in conjunction with an RCA 5819 photomultiplier tube and a 50-channel analyzer. Shielding and sample positioning arrangements for this counter were approximately the same as for the Geiger-Müller counter. Decay of an individual gamma ray peak could be followed by counting the sample periodically, plotting the gamma spectra, integrating under the desired peak, and plotting integrated counts as a function of time. This procedure is somewhat inaccurate if there are a large number of gamma rays present which can contribute to the desired gamma ray peak through Compton scattering. In general, however, if a peak is well defined its decay may be followed satisfactorily.

B. Calculation of Disintegration Rates.

When calculating cross sections in a study of this kind it is necessary that the absolute disintegration rate be obtained for each nuclide of interest in each of the samples. The observed counting rate is not equal to the disintegration rate of the sample but must be corrected for various factors which affect the observed count.

This may be expressed by:

$$D = \frac{A_{\text{obs}}}{f_a f_{\text{eff}} f_g f_{\text{bks}} f_{\text{abs}} f_{\text{ssa}}}$$

where D is the absolute disintegration rate, A_{obs} is the observed counting rate, and the factors are as follows: f_a , correction for abundance; f_{eff} , correction for counting efficiency; f_g , geometry correction; f_{bks} , backscattering correction; f_{abs} , correction for air and window absorption; f_{ssa} , correction for selfscattering and absorption in the sample. Obviously it is desirable that these factors be kept as close to unity as is possible. When samples of macroscopic size must be counted in instruments which have less than 100 percent geometry, those factors begin differing rather widely from unity. It is therefore necessary that they be known accurately if precise absolute beta counting is to be achieved.

f_a : Correction for Abundance:--When a nuclide decays it is quite possible, indeed probable, that the radiation it emits is a complex mixture. Thus one nuclide may decay by emission of a beta particle of a single maximum energy with no gamma rays; another may decay by emission of two or more beta particles of different

energies and several gamma rays; while a third may decay by electron capture and emission of a large number of gamma rays, each of which may or may not be internally converted. The point is that each of the components of a nuclide's decay scheme is affected to a different degree by the factors used to convert observed counting rate to absolute disintegration rate. When a nuclide with a complicated decay scheme is counted, it is necessary that the abundance of each of the various components of decay be known so that each may be corrected separately for each of the factors. The total "counting efficiency" or conversion factor for a given nuclide may then be obtained by adding the counting efficiencies of the various components of the decay.

For a majority of nuclides observed in this study the decay schemes are known and abundances for modes of decay have been published.¹⁸ In a number of cases, however, where the nuclide had not been studied thoroughly or was newly discovered in these bombardments, abundances were not available. When such cases occurred assumptions about the abundances were made. These assumptions will be stated subsequently in those sections which deal with each nuclide involved. Thus corrections to the calculated cross sections may be made when more complete data on abundances become available.

f_{eff} : Correction for Counting Efficiency:--Radiation counting instruments will usually have different counting efficiencies for different kinds of radiation and will often have different counting efficiencies for different energies of the same kind of radiation. In these studies it was assumed that 100 percent of beta particles

entering the sensitive volume of the Geiger-Müller tube would be counted. When x-rays or gamma rays were present counting efficiencies in the GM tube were obtained from the work of Studier and James.¹⁹ These efficiencies ranged from 0.5 percent for x-rays and gamma rays below 400 keV to 3.0 percent for 3 MeV gamma rays.

When gamma spectra were obtained on the 50-channel gamma pulse analyzer, the counting efficiency as a function of gamma energy was obtained from the work by Maguire and O'Kelley,²⁰ and Kahn and Lyon.²¹

f_g: Geometry Correction:--A simplification is often possible in these fission studies. When the monitor foil and the sample are both counted in the same counter in the same position, the geometry factor cancels out of the equations and need not be applied. If the monitor and sample are counted on different counters or in different geometries, however, the factors for each must be determined. This may be done by first counting a sample in a counter of known geometry, then counting in the desired counter, and comparing the two values.

For the Geiger-Müller counter a pure carrier-free beta particle emitter mounted on extremely thin foil is first counted in a 4π counter, then in the GM counter. A 3 percent geometry has been obtained for the "shelf 2" counting arrangement in which a great majority of these samples were counted.

Geometry correction factors for the gamma pulse analyzer were obtained by counting the alpha particles from a sample of Am^{241} under 52 percent geometry, then counting the 60 keV gamma ray on the analyzer. Using an abundance of 0.4 gamma rays per alpha particle, the geometry for each shelf arrangement in the analyzer could be calculated.

f_{bks} : Backscattering Correction Factor:--If a weightless sample be placed on a mounting plate which has a macroscopic mass, the observed activity will be higher than if there were no mass present. This increase due to backscattering of beta particles has been shown to be a function of the energy of the beta particle and the thickness and atomic number of the backing material.^{22,23} For a given beta particle maximum energy and a given backing material f_{bks} will increase with increasing backing thickness until a "saturation" thickness is reached, after which f_{bks} remains constant. For a given beta particle energy and thick backing materials, the f_{bks} will increase with increasing Z of the backscatterer. For a saturation thickness of a given Z and with varying beta particle energies, f_{bks} will increase from 0 to 600 kev and will remain approximately constant for all higher energy beta particles. In order to minimize errors due to the application of backscattering corrections almost all samples were mounted on aluminum plates thick enough to give saturation backscattering for all beta particles involved.

Since the magnitude of f_{bks} for saturation thicknesses of aluminum differs in the two references quoted, it was necessary to measure the factors empirically under the geometry used in these experiments. Data for several activities used by each of the authors plus others which were available in this laboratory indicated close agreement with the data of Burtt. Therefore his correction factors were applied for all samples.

Seliger²⁴ has shown that backscattering corrections for positrons are slightly smaller than for beta particles. His data are

fragmentary, however, and could not be applied with accuracy to these samples. Therefore, when positrons were encountered, correction factors for beta particles were used directly.

Because of the marked differences in energy distribution between beta particles having a given maximum energy and conversion electrons with that same energy, it is obvious that scattering and absorption factors obtained for beta particles may not be used for conversion electrons with any accuracy. Since these factors were not available for conversion electrons, it was customary to count through absorbers which would block out the conversion electrons whenever they were known or suspected to be present in the samples.

f_{abs} : Correction for Air and Window Absorption:--In the "shelf 2" geometry in which most of the samples were counted, radiation had to pass through approximately 5.8 mg/cm^2 of air and mica before entering the sensitive volume of the GM tube. This thickness of material would have a negligible effect on x-rays and gamma rays but could easily absorb a significant fraction of beta radiation, especially of low energy. When a sample containing only one or two beta particles was being counted, this effect could be corrected for by running absorption curves with either aluminum or beryllium absorbers. Careful extrapolation of the initial portion of these curves would then give the fraction of soft radiation absorbed by air and window. A majority of samples, however, had too many beta particles in their decay to allow accurate extrapolation of the initial portion of their absorption curves. Under such conditions the air and window absorption correction factors were calculated from

the beta particle aluminum half-thickness data of Seelmann-Eggebert.²⁵

Comparison of correction factors calculated in this manner with those measured by absorption on tracer activities of known composition indicated close agreement between the two methods.

f_{ssa} : Correction for Self Scattering and Absorption in the

Sample:--When any but a weightless sample is counted, the radiation emitted may be scattered or absorbed by the mass of the sample itself.

The size of this effect will depend on the nature and energy of the radiation and on the thickness and atomic number of the sample.

Nervik and Stevenson²⁶ have measured this effect in samples of moderate thickness (0.20 mg/cm^2) and have shown that scattering may increase the observed counting rate of samples of this size by as much as 30 percent. For soft beta particles this scattering is soon counterbalanced by absorption in the sample and f_{ssa} drops below 1.00, but for a majority of beta particle energies and sample thicknesses in this range the correction factor is greater than one.

Samples for these self scattering experiments were especially prepared to have a uniform thickness over a fixed area. When samples are separated from a bombardment target it is usually impossible to get an absolutely uniform deposit on the counting plate; the powders or slurries will always tend to collect in small piles or in the corners of the dish. In order to minimize errors due to non-uniform samples, it was customary to adjust the sample thickness in such a way that the flattest portion of the f_{ssa} versus sample thickness correction curve applied.

Strictly speaking, the self scattering correction factors of Nervik and Stevenson apply only to the salts used (NaCl and $\text{Pb}(\text{NO}_3)_2$) on saturation thicknesses of stainless steel. The most accurate data may be obtained only by making specific measurements on each nuclide of interest in that chemical form in which it is to be separated after the bombardment. Since that is obviously impractical for the number of nuclides separated in these bombardments, the available data have been used to estimate f_{ssa} for those nuclides of interest. The correction factors are too large to be ignored and these data seem to be the most useful that have been published.

C. Calculation of Cross Sections

During a bombardment the rate of change of the number of atoms of a given nuclide may be expressed as

$$\frac{dN}{dt} = In\sigma - \lambda N$$

where N is the number of atoms of the nuclide of interest, I is the beam intensity in particles per cm^2 per unit time, n is the number of atoms in the target, σ is the formation cross section in cm^2 , and λ is the decay constant for the nuclide. Integration of this equation gives

$$\sigma = \frac{\lambda N}{\ln(1 - e^{-\lambda t})}$$

where t is the duration of bombardment. λN is the absolute disintegration rate at the end of bombardment and may be obtained by correcting the observed counting rate for chemical yield and for the various factors described in section 2.

When one cross section is obtained by comparison with an aluminum monitor, this equation becomes somewhat simpler; i.e.,

$$\sigma_1 = \frac{(\lambda N)_1}{(\lambda N)_2} \left(\frac{W_2}{W_1} \right) \left(\frac{M_1}{M_2} \right) \left(\frac{1 - e^{-\lambda_2 t}}{1 - e^{-\lambda_1 t}} \right) \sigma_2$$

where $(\lambda N)_1$ and $(\lambda N)_2$ are disintegration rates of the nuclide and Na^{24} , W_1 and W_2 are the weights of the target and aluminum foils, M_1 and M_2 the atomic weights of the target and aluminum, λ_1 and λ_2 the decay constants for the nuclide and Na^{24} , t is the duration of bombardment, σ_2 is the formation cross section for Na^{24} in the reaction $\text{Al}^{27}(p,3pn)\text{Na}^{24}$, and σ_1 is the desired cross section.

D. Nuclides Observed*

Sodium:--Sodium 24 was the only activity observed in the sodium fraction. Starting with approximately 1,000 counts per minute, the gross decay curve went down to background with a 15.1 hour half-life. An aluminum absorption curve indicated the presence of a 1.4 Mev beta particle while analysis of the gamma spectrum showed a gamma ray of 1.36 Mev, both of which have been reported for Na^{24} .

Magnesium:--The gross magnesium fraction decayed with a 21.2 hour half-life for over eight half-lives, then "tailed" into a long-lived component at 10 counts per minute above background. Aluminum absorption curve measurements indicated the presence of a 3 Mev beta particle with a softer component also present. This was

*Unless otherwise quoted, disintegration data were obtained from Hollander, Perlman, and Seaborg,¹⁸ or the Chart of the Nuclides.²⁷

confirmed by analysis of the beta spectrum on a crude beta ray spectrometer. The 21.2 hour activity has been identified as Mg^{28} , decaying by emission of a 300-400 kev beta particle. The 2.30 minute Al^{28} is in equilibrium with the Mg^{28} parent and decays by emission of a 3 Mev beta particle. The low long-lived tail may be attributed to a trace of Be^7 which could have followed through the magnesium chemistry.

Potassium:--The potassium decay curve consisted of two components which could be separated into 12.4 and 22.4 hour half-lives and which have been identified as K^{42} and K^{43} . Aluminum absorption curves indicated the presence of a beta particle of approximately 3.5 Mev belonging to the short-lived component and a softer beta particle of approximately 0.8 Mev with the longer-lived K^{43} .

Potassium 42 decays 75 percent by a 3.6 Mev beta particle and 25 percent by a 2.0 Mev beta particle while K^{43} has beta particles of 0.8 and 0.24 Mev reported but with no abundances. In calculating the K^{43} cross section, it was assumed that the nuclides decayed 80 percent by emission of the 800 kev beta particle and 20 percent by the 240 kev beta particle, this assumption being based on the shape of the soft components of the absorption curve. Analysis of the gamma spectra showed that there were two gamma rays present, one at 375 ± 10 kev and another at 615 ± 10 kev, each of which decayed with approximately a 22 hour half-life. Potassium 43 has a gamma ray of approximately 0.4 Mev reported, but this energy measurement was made by absorbers. It seems probable, therefore, that both the 375 and 615 kev gamma rays may be assigned to K^{43} . When corrected for

counting efficiency in the NaI crystal, the two gamma peaks have the same abundances, within experimental error. No evidence of the 1.51 Mev K^{42} gamma ray was seen in the spectra, probably because of its low abundance and low counting efficiency.

Chromium:--Gross decay of the chromium fraction showed the presence of a small amount of a short-lived activity which may have been 42 minute Cr^{49} . The curve then tailed into a long-lived component, part of which may have been 27 day Cr^{51} and part a longer-lived nuclide. The activity level of the chromium fraction, however, was too low for accurate identification of any of these species, although gamma rays of approximately those energies reported for Cr^{51} were observed. Cross sections for these two nuclides would be very uncertain because of this lack of positive identification and have therefore not been included in the tabulated data.

Manganese:--The gross manganese fraction decayed over 8 half-lives in a 2.6 hour line, then tailed into a small amount of 6 day activity, and finally into a very long-lived component at approximately 10 counts above background. The gamma spectrum contained a fairly large number of gamma ray peaks, some of which could be assigned as those reported for 2.6 hour Mn^{56} or 6.0 day Mn^{52} . Since the possibility of the appearance of Compton scattered peaks was so great, the complete identification of either spectrum or the unequivocal assignment of all peaks in the observed spectrum was quite impossible. From the peaks identified and the observed half-lives, however, it seems that Mn^{52} and Mn^{56} were present in high purity. The long-lived tail may have been 310 day Mn^{54} or possibly

a small amount of impurity in the sample; the activity level was too low for identification.

Iron:--The iron fraction decayed in a straight line with a half-life of 46 days. Initial activity of these samples was approximately 1,500 counts per minute after a 2 hour, thick target bombardment. On several bombardments in which special pains were taken to ensure an iron fraction purified from all possible contamination, no trace was seen of any activity which could be assigned to the 8.4 hour Fe^{60} which has been reported. If this nuclide had been correctly reported in the literature, and if it were to have a counting efficiency comparable to that of 46 day Fe^{59} , it should have been formed in sufficient quantity in these bombardments to be easily seen and identified. It would seem, therefore, that the mass assignment of Fe^{60} in the literature is incorrect.

Cobalt:--An activity which decayed over 9 half-lives with a half-life of 1.65 hours was present in the cobalt fraction. The gross decay curve then tailed over into a very long-lived component (>60 days) at approximately 50 counts above background. Aluminum absorption curves showed a beta particle of approximately 1.1 Mev to be present in the 1.65 hour component. Cobalt 61 is reported to decay 55 percent by a 1.45 Mev beta particle and 45 percent by a 1.00 Mev beta particle, and it should not be expected that an absorption curve would separate them.

Gamma spectra showed the presence of annihilation radiation and a gamma ray of approximately 830 kev in the long-lived tail of the cobalt fraction. The 72 day Co^{56} , 270 day Co^{57} , and 72 day Co^{58} each

decay by positron emission, while Co^{56} has a gamma ray of 845 kev and Co^{58} a gamma ray of 810 kev. Therefore abundances of these nuclides could not be obtained from the gamma spectra. Since it was equally impractical to separate these activities on the low counting GM decay curve, their cross sections have not been included in the final tabulation.

Nickel:--A two component decay curve of 2.56 hour and 56 hour activities was obtained in the gross nickel fraction, corresponding to Ni^{65} and Ni^{66} respectively. Aluminum absorption curves taken after the short-lived Ni^{65} had decayed showed a hard component of approximately 2.7 Mev and a softer component of approximately 0.3 Mev. A 2.63 Mev beta particle is reported for the 5.1 minute Cu^{66} , daughter of Ni^{66} . In calculating cross sections, it was assumed that Ni^{66} decayed 100 percent by emission of the 300 kev beta particle.

Copper:--Nuclides of 12.9 and 60 hour half-lives were the only ones detectable in the copper fraction. These were assumed to be Cu^{64} and Cu^{67} , respectively. No evidence was seen of the neutron deficient 3.3 hour Cu^{61} although purified samples were counted less than 6 hours after the end of bombardment.

Gallium:--The gross gallium decay curve contained two activities, of 5.0 hour and 14.3 hour half-lives, which were definitely resolvable. In addition, there was a small amount of a short-lived activity which may have been 20 minute Ga^{70} but which could not be identified accurately because of the relatively larger amounts of other activities present. Since purification of the gallium fraction took slightly more than two hours (or six half-lives of Ga^{70}) from the end of

bombardment, a large part of this original activity decayed before the fraction could be counted. Aluminum absorption curves confirmed the presence of a beta particle of approximately 1.5 Mev which was associated with the 5 hour activity. The two activities seen are assumed to be 14.3 hour Ga⁷² and 5.0 hour Ga⁷³.

Arsenic:--After decay of short-lived activities was complete, the gross arsenic fraction decayed to background with a 17.5 day half-life. When this activity was subtracted from the gross curve a curve was obtained which could not be visually resolved into straight components. Assuming that the second curve consisted of 26.8 hour As⁷⁶ and 39 hour As⁷⁷, however, an analytical "Biller Plot" was used to separate the activities. Aluminum absorption curves could not be used in this case to identify individual nuclides but did show beta particles of approximately those energies reported for As⁷⁴, As⁷⁶, and As⁷⁷.

Bromine:--Resolution of the gross decay curve of bromine gave activities of three half-lives: 2.4 hour, 4.4 hour, and 35 hour; where the decay was followed from an initial count of approximately 16,000 counts per minute down to 10 counts above background. Aluminum absorption curves showed the presence of beta particles of approximately 1.8 and 0.6 Mev. No gamma spectra were taken since equipment was not available when these bombardments were run. On the basis of these data, the activities were assumed to be 4.58 hour Br⁸⁰ in equilibrium with the 18 minute Br⁸⁰, 35.9 hour Br⁸², and 2.4 hour Br⁸³.

Rubidium:--The rubidium fraction decay curve consisted of a small amount of activity of approximately 5 hour half-life, and a mixture of activities having half-lives of approximately 20 days. A Biller Plot was used to separate the long-lived component, assuming that it was made up of 19.5 day Rb^{86} and 34 day Rb^{84} . Since there was a good possibility that 4.7 hour Rb^{81} and 6.3 hour Rb^{82} could have been formed by spallation of the niobium impurity in the target the short-lived component of the rubidium curve was ignored in calculating cross sections. Using a value of 0.1 percent as niobium impurity in the tantalum target, and estimating a cross section of 5 millibarns for the reaction $\text{Nb}^{93}(\text{p},5\text{p}5\text{n})\text{Rb}^{84}$, it is estimated that niobium could have contributed no more than 5 percent of the cross section actually observed for Rb^{84} . Of all the activities reported here, the Rb^{84} should have had the greatest error due to niobium present in the target material.

Strontium:--The gross strontium fraction decay curve was resolvable into 9.7 hour and 38 hour activities and a long-lived component which had a half-life greater than 30 days. Aluminum absorption curves showed the presence of hard beta particles such as those reported for 9.7 hour Sr^{91} . The 38 hour activity was presumed to be Sr^{83} , but since this nuclide is in the region of highest yields in the spallation of niobium its cross section is not included in the tabulated data. When all of the short-lived components had had time to decay, yttrium was milked from the strontium sample, the strontium was remounted, and decay of both samples was followed. The repurified strontium fraction decayed with a 54 day half-life and aluminum

absorption curves showed the presence of the 1.5 Mev beta particle reported for Sr^{89} , while the yttrium fraction decayed with approximately 60 days and also contained a beta particle of 1.5 Mev. The 61 day Y^{91} should have grown in from 9.7 hour Sr^{91} and cross sections for Sr^{91} were calculated on that basis.

Zirconium:--Activities with half-lives of 17 hours, 80 hours, and approximately 65 days could be resolved in the zirconium gross decay curve. Aluminum absorption curves showed the presence of beta particles of approximately 0.96 Mev. These were probably due to the 0.91 Mev positrons of 78 hour Zr^{89} . This nuclide undoubtedly has one of the higher cross sections for formation in the spallation of niobium; therefore, it is not included in the tabulated data. The 17 hour activity could be due either to Zr^{86} or Zr^{97} , while the long-lived component might have been either 85 day Zr^{88} or 65 day Zr^{95} . The neutron deficient isotopes, however, would be expected to have very much lower counting efficiencies than the beta particle emitting neutron excess nuclides. Therefore, the assumption has been made that all of the 17 hour and 65 day activities observed were due to Zr^{97} and Zr^{95} , respectively. The cross sections obtained on this basis then represent upper limits to the true cross section.

Molybdenum:--The molybdenum decay curve could be resolved into two activities with half-lives of 6.7 and 67 hours. The 6.7 hour isomer of Mo^{93} would be formed in very high yield as a spallation product of niobium, so its cross section has not been included in the tantalum data. Beta-spectrograph curves confirmed the presence of the 1.2 Mev beta particle of 67 hour Mo^{99} .

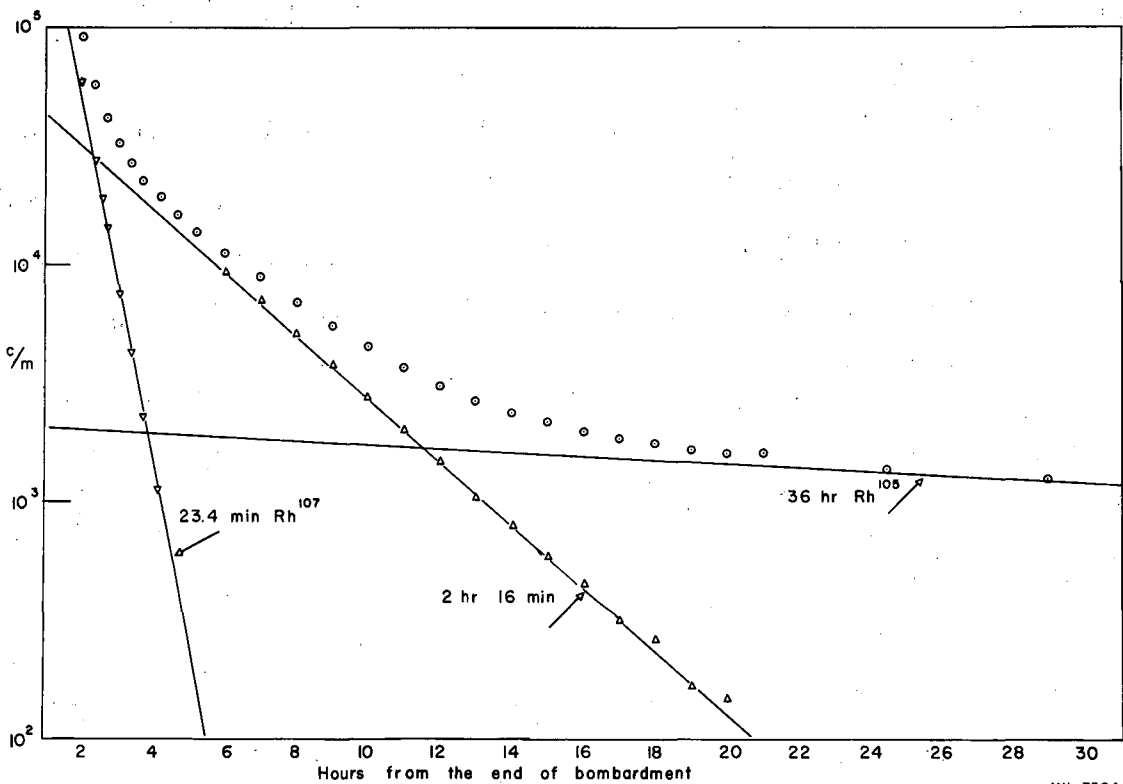
Ruthenium:--Ruthenium which was separated immediately after bombardment gave a decay curve which could be resolved into activities having half-lives of 4.5 hours, 36 hours, and 51 days. Aluminum absorption curves taken 2.5 hours from the end of bombardment showed the presence of the 1.1 Mev beta particle of 4.5 hour Ru^{105} . Cross sections for Ru^{105} were calculated both on its resolution in the decay curve and resolution of its 36 hour Rh^{105} daughter. The 41 day activity was presumed to be Ru^{103} although its activity level was not high enough for accurate identification with absorption curves of the beta-spectrometer.

On bombardments in which all of the 4.5 hour Ru^{105} had been allowed to decay before the ruthenium was purified, the decay curve could be resolved into components of 40 days and 2.8 days half-life. Presumably the 2.8 day activity was Ru^{97} . Since the nuclide decays by electron capture, however, its counting efficiency in the GM counter would be both low and uncertain. Therefore decay of these samples was also followed on the gamma pulse analyzer. The 217 kev gamma ray reported for Ru^{97} showed up quite clearly in the spectra and it decayed with approximately a 2.8 day half-life. No abundances for the 217 kev gamma ray have been reported. In calculating the Ru^{97} cross sections, it was assumed that 100 percent of the decay was with emission of a 217 kev gamma ray and that there was no conversion. Thus the value obtained should represent a lower limit on the Ru^{97} cross section.

Rhodium:--The gross decay curve of rhodium could be separated into components of 2 hour 16 minutes and 36 hour half-lives.

Beta-spectrograph curves showed a beta particle of approximately 1 Mev to be associated with the short-lived activity while a beta particle of 0.6 Mev was seen after all of this short-lived activity had decayed. The 36 hour 0.6 Mev beta particle emitter was presumed to be Rh^{105} . No 2 hour 16 minute beta particle emitter had previously been reported for rhodium. A consideration of the chemical separation and purification procedure used for rhodium showed that no element other than iridium could have been present in the final sample. Iridium activities could not have been formed in any significant amounts in the tantalum bombardments. Comparison of formation cross sections of this activity with those of Rh^{105} indicated that the nuclide probably had a mass greater than 105.

In order to investigate this new activity further, a series of bombardments were run in which uranium was bombarded with 340 Mev protons. In one of these the target material was bombarded for four minutes. Ruthenium was separated within three minutes of the end of bombardment and allowed to decay. Rhodium was then separated from both the original target solution and the ruthenium fraction. A 25 minute Rh^{107} , 36 hour Rh^{105} , and the 2 hour 16 minute activity were seen in the rhodium removed from the original target solution while only the 25 minute and 36 hour activities had grown from ruthenium parents. The three component decay curve obtained in these bombardments is shown in Figure 4. Special steps were taken in these separations to ensure that no iridium was present. Assuming the new activity to have the same counting efficiency as Rh^{105} these decay curves showed the new nuclide to have a higher formation cross section than Rh^{105} in the uranium bombardments.



MU-7384

Figure 4. Decay curve of the rhodium fraction separated from uranium.

Gamma spectra were obtained on rhodium samples separated from both tantalum and uranium and indicated a large number of gamma rays associated with decay of the 2 hour 16 minute activity. Resolution of the pulse analyzer curves makes abundance data very uncertain but it seems probable that gamma rays of 195, 225, 510, 630, 715, 1060, 1200, 1260, and 1500 kev are present in the decay scheme of the new activity.

Assignment of a mass to this new activity cannot be made unequivocally. Cross section data on both tantalum and uranium indicate that the activity is heavier than Rh^{105} . The ruthenium milking experiment shows that it is not the daughter of a ruthenium parent which has a half-life greater than 1 minute. Several of the gamma rays have energies close to those reported for 30 second Rh^{106} , but if we take the maximum gamma ray energy and the beta particle energy we get a Q value of only 2.5 Mev. The reported Q value for Rh^{106} is 3.53 Mev and it seems most unlikely that a 136 minute isomer of Rh^{106} could exist. On the basis of present data it seems more probable that the 136 minute activity is an isomer of Rh^{107} which is not involved in the decay of 4 minute Ru^{107} . Attempts have been made to separate this nuclide on a time-of-flight isotope separator but they were not successful because of difficulties in ionizing the rhodium samples.

As part of the uranium bombardments, spectra of gamma rays associated with the 25 minute Rh^{107} were obtained. These were superimposed on the 136 minute and 36 hour activities so that accurate

abundances could not be calculated. Gamma rays of 95 ± 5 , 145 ± 5 , 305 ± 5 , 390 ± 10 , and 475 ± 10 kev were observed to decay with approximately a 25 minute half-life.

Decay curves of rhodium samples which had been separated from the tantalum targets after all 136 minute activity had decayed out could be resolved into three components: a large amount of 36 hour Rh^{105} , a small amount of 4.5 day activity, presumably Rh^{106} , and a long-lived component of approximately 200 day half-life, probably Rh^{103} . Decay of gamma spectra was also followed in these samples. Both Rh^{105} and Rh^{101} have gamma rays of approximately 300 kev reported, but by resolution of the decay curve of the 300 kev gamma ray, it was possible to obtain cross sections for Rh^{101} . No abundances have been reported for the 300 kev gamma ray in Rh^{101} , however, so in these calculations it was assumed that 100 percent of the decay included the 300 kev gamma ray and that no conversion took place. The value obtained is therefore a lower limit to the actual cross section.

Palladium:--The only activities observed directly in the gross palladium fraction were the 13.1 hour Pd^{109} and a small amount of activity which could have been 17 day Pd^{103} . Palladium 103 decays by electron capture with no gamma rays reported. The amount of 17 day activity present was too low to allow counting of x-rays through absorbers in the GM tube and attempts to follow decay of the x-rays in the pulse analyzer were not successful.

No evidence was seen in the gross palladium decay of 5.5 hour Pd^{111m} , 22 minute Pd^{111} , or 21 hour Pd^{112} . A 7.5 day Ag^{111} was

observed to grow into a target solution from which all silver had been removed immediately after bombardment. On the basis of this information the total cross section for Pd^{111} could be calculated; but since both of the Pd^{111} isomers decay to Ag^{111} calculation of isomer cross sections by this method would be somewhat uncertain.

Silver:--Activities of 5.3 hour Ag^{113} , 3.2 hour Ag^{112} , 7.5 day Ag^{111} , and 210 day Ag^{110} were resolvable in the gross silver decay curve. The 7.5 day and 270 day activities were easily resolved, but a Biller Plot was necessary to separate the 3.2 and 5.3 hour activities. Absorption curves taken when the activity was primarily Ag^{111} showed a 1 Mev beta particle with no soft component which would be attributed to conversion electrons from 8.3 day Ag^{106} .

Gamma spectra taken after almost all of the 7.5 day activity had decayed and before the gross decay curve became an exactly 270 day half-life showed the presence of gamma rays of 63, 154, 280, and 350 kev, all of which have been reported for 40 day Ag^{105} . Cross sections for this nuclide were based on the 280 kev peak, assuming that the 280 kev gamma ray was 25 percent abundant and unconverted.

Gamma spectra taken after most of the 40 day Ag^{105} had decayed showed peaks at 660, 760, 935, and 1400 kev, all of which have been reported for 270 day Ag^{110} . Calculations of the Ag^{110} cross section were based on the amount of the 660 kev gamma radiation and using its reported abundance of 100 percent and e/γ ratio of 0.0025.

Cadmium:--Activities of 43 days, 53 hours, and 6.7 hours were resolved in the gross cadmium decay curve, corresponding to Cd^{115m} , Cd^{115} , and Cd^{107} respectively. The Cd^{115} and Cd^{115m} isomers decay by

emission of beta particles of known energies so cross sections could be calculated for these nuclides fairly easily. Cadmium 107 decays more than 99 percent by electron capture and emission of a 94 keV gamma ray so that a cross section based on raw GM counts would be subject to fairly large errors. Therefore, decay of cadmium samples was also followed on the gamma pulse analyzer and cross section calculations for Cd^{107} based on the abundance of the 94 keV peak and the reported e/γ ratio of 16.

The 57 minute Cd^{105} could not be identified in the gross cadmium fraction because of the large abundance of other activities present. In order to determine whether any of this activity had been formed, an experiment was run in which silver was removed from the target solution immediately after bombardment. Cadmium 105 was allowed to decay for two days, then silver was again removed and purified. Decay of this silver sample was then followed to see if any Ag^{105} had grown in from the Cd^{105} parent. While the gross GM counter decay curve did seem to show an activity of approximately 40 day half-life at about 10 counts above background, none of the Ag^{105} gamma peaks could be identified. Therefore, it must be concluded that Cd^{105} is not formed in sufficient quantities to be detected by this method.

Gamma spectra taken after most of the 43 day Cd^{115m} had decayed confirmed the presence of the 87 keV gamma ray associated with 470 day Cd^{109} . The activity level was so close to background, however, that no very accurate value for the abundance of this gamma ray could be determined. Cross sections for this nuclide are therefore not included in the final tabulation.

Indium:--A long-lived component of 50-day half-life was present as a tail on the gross indium decay curve. Aluminum absorption curves showed the 2 Mev beta particle of 49 day In^{114} to be in this activity. Shorter-lived components were also present in the sample but since 4.3 hour In^{109} , 5.0 hour In^{110m} , 1.74 hour In^{113m} , and 4.5 hour In^{115m} were all expected to be formed in some degree they could not possibly be separated in the gross GM decay curve. Indium samples were followed in the gamma pulse analyzer and cross sections for those nuclides that could be identified were based on the gamma spectrum.

The 205 kev gamma ray reported for In^{109} was observed to decay with a 4.3 hour half-life. No abundance data were available for this gamma ray; in the calculations it was presumed to be present in 100 percent abundance and to be unconverted.

The 935 and 661 kev gamma rays of In^{110m} were seen to decay with approximately a 5 hour half-life. Both are reported to be in 100 percent abundance. The e/γ ratio is 0.005 for the 660 kev gamma ray and it was assumed that the 935 kev line was also unconverted.

An activity of 2.8 day half-life could be separated in the gross GM counter decay curve, and was presumed to be 2.8 day In^{111} , but since this nuclide decays essentially 100 percent by electron capture the GM data were not used in calculating this cross section. Gamma rays of 247 and 172 kev were seen in the gamma spectra and decayed with approximately a 2.8 day half-life. In In^{111} the 172 and 247 kev gamma rays are 100 percent abundant and have conversion coefficients of 0.12 and 0.064, respectively.

Tellurium:--The gross decay of the tellurium fraction could be separated into activities having half-lives of 2.8 hours, 4.5 days, and 17 days, corresponding to Te^{117} , Te^{119} , and Te^{121} , respectively. No data were available for the abundance of the 2.5 Mev positron reported for Te^{117} . In the calculations it was assumed that this nuclide decayed 100 percent by emission of a positron, with a 28 hour Sb^{117} daughter decaying 100 percent by electron capture.

Cesium:--Activities having half-lives of 6.2 hours, 31 hours, and 34 days were the only ones detectable in the gross cesium decay curve. These would correspond to Cs^{127} , Cs^{129} , and Xe^{127} , respectively.

Gamma spectra showed the presence of the 65, 125, and 416 kev gamma rays reported²⁸ for Cs^{127} and they were seen to decay with approximately a 6 hour half-life. The 57 kev gamma ray reported for Xe^{127} was observed as part of the 34 day component. Since the positron abundances in Cs^{127} have not been reported, the cross section calculations for Cs^{127} were based on the 57 kev gamma ray in its Xe^{127} daughter. Here the nuclide decays 100 percent by electron capture and it was assumed that there was one 57 kev gamma ray per disintegration.

The 31 hour Cs^{129} decays completely by electron capture, therefore the gross GM decay data could not be used in calculating its cross section. Wapstra²⁹ has reported gamma rays of 385 and 560 kev as belonging to this nuclide. Gamma spectra taken on the gross cesium fraction after all of the 6 hour Cs^{127} had decayed showed the presence of gamma rays of 375 ± 10 and 585 ± 20 kev, each of which decayed with a 31 hour half-life. In addition, the 375 kev peak was deformed in such a way as to indicate the presence of a small amount of a gamma

ray of approximately 420 ± 10 kev. Correcting the 375, 420 and 585 kev gamma rays for counting efficiencies of 42, 34, and 17 percent, respectively, the gamma ray abundances are in the approximate ratio 1.0, 0.092, and 0.233. The Xe^{129} daughter has a gamma ray of 40 kev reported, and it is possible that it and the 375 kev gamma ray are in coincidence while the 420 kev gamma ray is a crossover transition. The 40 kev gamma ray is very highly converted, however, so that it would be easily missed in the gamma spectra.

The 375 and 420 kev peaks could not be easily resolved in the gamma spectra. In calculating cross sections for Cs^{129} the combined peak was used. It was assumed that these gamma rays were unconverted and were present in 82 percent of the disintegrations of Cs^{129} .

No evidence could be seen of either the 9.6 day Cs^{131} , or 7 day Cs^{132} in the gross GM decay curve. Each of these nuclides decays by electron capture, Cs^{131} with no gamma rays, and Cs^{132} with a gamma ray of 685 kev.²⁷ They would therefore have a very low counting efficiency in the GM counter. A gamma peak was observed at approximately 680 kev, but it was not in great enough abundance for a good half-life to be obtained.

Barium: --Activities corresponding to 2.0 hour Ba^{129} , 2.4 day Ba^{128} , and 12 day Ba^{131} were observed in the gross barium decay curve. Aluminum absorption curves taken when the 2.4 day activity was predominant showed the presence of a beta particle of approximately 3 Mev, presumably the 3.0 Mev positron emitted by the cesium daughter of Ba^{128} . Gamma spectra taken when the 12 day activity was predominant showed the 122, 214, 241, 370, and 494 kev gamma rays reported for Ba^{131} .

In calculating cross sections for Ba¹²⁸ the decay scheme of Lindner³⁰ was used. According to these data, 2.4 day Ba¹²⁸ decays 100 percent by electron capture while its 3.8 minute Cs¹²⁸ daughter decays 71 percent by emission of a 3.0 Mev positron and 29 percent by electron capture.

Barium 129 was assumed to decay 100 percent by the 1.6 Mev positron reported by Fink and Wiig.³¹

Barium 131 decays completely by electron capture; cross sections for this nuclide were calculated on the number of cesium x-rays seen in a single channel gamma pulse analyzer using a NaI crystal.

Cerium:--Activities having half-lives of 6.3 hours, 16 hours, and 72 hours were resolved in the cesium decay curve. These were assumed to be Ce¹³³, Ce¹³⁴, and Ce¹³⁵, respectively. There was also a long-lived tail of very low abundance (less than 10 counts per minute) which may have been due to 36 day Ce¹⁴¹, but the activity level was too low for an accurate half-life to be determined. Aluminum absorption curves taken 5 hours after bombardment showed the presence of beta radiation of approximately 2.4 Mev, probably the 2.7 Mev positron reported for the 6.3 minute La¹³⁴ daughter of Ce¹³⁴. In calculating cross sections for the cerium isotopes, the data on decay energies and abundances by Stover³² were used.

The Rare Earths:--After several bombardments in which the heavy rare earths were separated and their decay followed, it became apparent that published data on the neutron deficient isotopes of these elements was quite incomplete. A program was then begun to get more accurate mass assignments, half-lives, and decay characteristics

of isotopes of these elements formed in the tantalum bombardments. In general, the procedures used in this program were as follows: 1. The heavy rare earths were separated after a low level bombardment and their gross decay followed. This gave an indication of the half-lives and approximate abundances of the activities present in each element. 2. High level bombardments were run in which attempts were made to have at least 10^8 counts per minute of each nuclide present after chemical purification. The chemical steps were carried out essentially carrier-free (usually about 20 micrograms of carrier were added). After the elements had been chemically separated the activities present were mass separated on a time-of-flight isotope separator.³³ Thus accurate mass assignments could be made for the activities seen in the gross decay of each element. The time-of-flight machine is not a very efficient instrument, however, mainly because of the problems involved in ionizing the sample material. It was found that only nuclides of the four heaviest rare earths could be made from tantalum in sufficient quantities for separation by this method. 3. When possible, decay characteristics were obtained on isotopically separated samples. Otherwise they were taken in the gross mixture under the most favorable conditions. In those cases where a daughter activity of sufficiently long half-life was present a second column separation milking was run to confirm presence of the daughter.

No information on abundances of gamma rays, positrons, or conversion electrons for most of the rare earth nuclides formed in the spallation of tantalum was available in the literature. Rather than make assumptions as to the abundance of these modes of decay, the

samples were counted on the Geiger counter. Counts were taken through sufficient absorber (972.6 mg Al/cm²) to block out all beta particles, positrons, and conversion electrons but not thick enough to absorb a significant fraction of the gamma radiation. In the cross section calculations for these nuclides the counting efficiency was assumed to be 1 percent for each activity (or 2 percent for a parent and daughter in equilibrium).

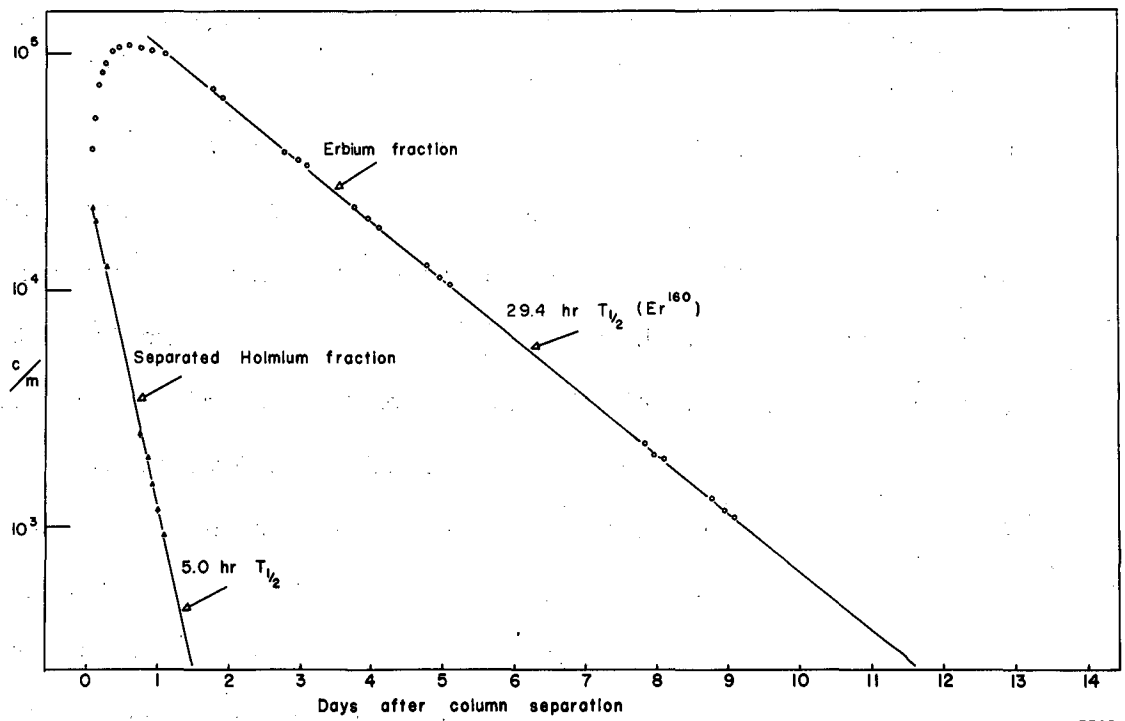
Erbium:--Neutron deficient activities of erbium reported in the literature at the time the rare earth program was begun were ~17 hour Er¹⁶¹, ~65 hour Er¹⁶³, and 10 hour Er¹⁶⁵. The gross decay curve of erbium could be resolved into activities of 183 minutes and 29 hours half-life. No evidence was seen for any of the three activities previously reported. Separation on the time-of-flight instrument showed the 29 hour activity to be Er¹⁶⁰, while the 183 minute activity was Er¹⁶¹.

Handley and Olson³⁴ have recently reported Er¹⁶¹ as having a 3.6 hour half-life and a holmium daughter of 2.5 hour half-life. They report gamma rays of 195, 824, and 1120 kev for the parent and 90 kev for the daughter. They also report no annihilation radiation and say that positrons, if present, constitute only a small fraction of the decay. Analysis of the gross erbium fraction for beta radiation on a crude beta-ray spectrometer showed the presence of positrons of 1.2 ± 0.1 Mev which decayed with approximately a 3 hour half-life. No attempt was made to milk the holmium daughter of Er¹⁶¹ so that the positron may belong to either Er¹⁶¹ or Ho¹⁶¹.

The 29 hour Er^{160} is a new activity which has not previously been reported. Decay curves of the gross erbium fraction separated immediately after bombardment and isotopically separated Er^{160} both showed a straight 29 hour half-life with no growth present. When an erbium fraction which had been separated immediately after bombardment had been allowed to decay for several days, however, and a second erbium-holmium column separation made, the erbium fraction showed a decided growth before decaying with a straight 29 hour line, while the holmium fraction decayed with a half-life of 5.0 hours. (See Figure 5.) Gamma rays of approximately 87, 194, 650, 730, 890, and 970 kev plus x-rays of 46 kev were seen in the holmium fraction. They also were seen to grow into the erbium sample. No gamma rays or annihilation radiation were observed which could be assigned to Er^{161} .

Handley³⁵ has recently reported a 5.0 hour holmium activity having gamma rays of 190, 710, and 950 kev which was formed by proton bombardments on Dy_2O_3 . The activity was assigned to Ho^{162} on the basis of abundance measurements relative to the 2.5 hour Ho^{161} formed in the same bombardments. From the half-life and gamma spectra measurements, it would seem that this is the same activity as was milked from Er^{160} and that it actually is Ho^{160} instead of Ho^{162} .

Handley and Olson³⁶ have reported a 75 minute activity for Er^{163} . No evidence was seen of this activity in gross erbium fractions which were counted within six hours of the end of bombardment, although it may have been obscured by the 183 minute Er^{161} . Attempts to separate Er^{163} on the time-of-flight instrument and to milk it from any possible long-lived Tm^{163} parent were unsuccessful.



MU-7385

Figure 5. Er^{160} - Ho^{160} decay curve.

No evidence of 10 hour Er^{165} was seen in the erbium gross decay curve and attempts to separate it isotopically were unsuccessful. For reasons which will be explained later, Er^{165} should not be formed in large enough abundance from tantalum to be separated isotopically. The gross erbium decay curve included a 2.5 hour daughter growing into a 3.1 hour parent and a 5 hour daughter growing into a 29 hour parent so it is not surprising that a relatively small amount of a straight 10 hour activity could not be resolved.

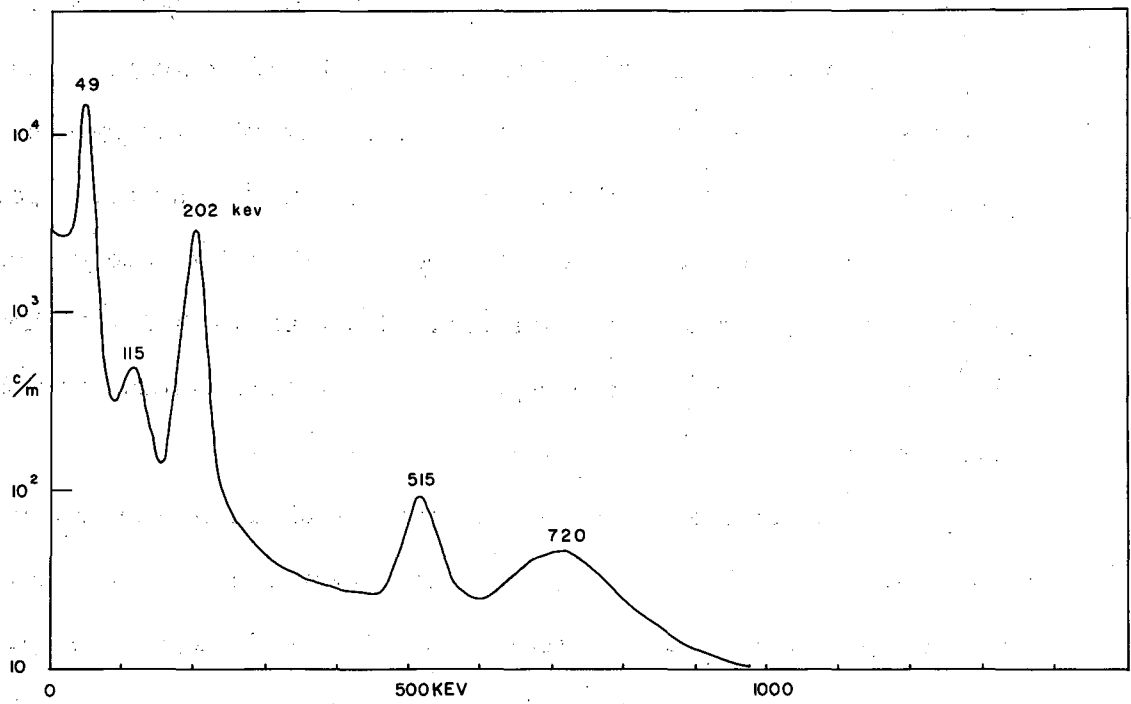
Thulium: -- Neutron deficient activities previously reported for thulium are 7.7 hour Tm^{166} , 9.6 day Tm^{167} , and 85 day Tm^{168} . In the decay of the gross thulium fraction the 7.7 hour and 9.6 day activities could be resolved. In addition, an activity of approximately 29 hours was seen. The activities were separated isotopically and the mass assignments of the 7.7 hour and 9.6 day activities were found to be correct. The 29 hour activity was identified as Tm^{165} . As a further check on this mass assignment a sample of thulium which had been separated immediately after bombardment was allowed to decay for three days. A thulium-erbium column separation was then run. The erbium fraction decayed with the 10.2 hour half-life expected of the Er^{165} daughter of Tm^{165} . Handley and Olson³² have recently reported Er^{165} to have a half-life of 24.5 hours. The discrepancy between these half-lives is probably due to resolution of the multicomponent decay curves in each case.

Unequivocal assignment of gamma ray energies was not made for these nuclides in the gross thulium fraction. Thulium 167, however, was obtained pure by milking it from its Yb^{167} parent. The 7.7 hour

Tm^{166} daughter of Yb^{166} was also present initially. After the 7.7 hour Tm^{166} had decayed the sample decayed with a straight 9.6 day half-life. A gamma spectrum taken on this activity showed gamma rays of 49, 115, 202, 515, and 720 keV to be present in relative abundances of 1, 0.02, 0.29, 0.09, and 0.18, respectively, after correction for counting efficiency in the NaI crystal had been made. This spectrum is shown in Figure 6.

Thulium 166 and Tm^{167} both have parent activities of moderate half-lives. Since the chemical purification and column separation take approximately six hours from the end of bombardment, cross sections for these nuclides could be seriously affected by decay of the parents. In those bombardments from which thulium cross sections were obtained, the rare earth fraction was allowed to decay overnight before the column separation was run. Cross sections for 29 hour Tm^{165} and 9.6 day Tm^{167} then represent total chain yields for their mass numbers.

No 85 day activity was seen in those thulium samples mounted for cross section counting. In one of the survey bombardments, however, when decay of a very active thulium sample was followed, the 9.6 day Tm^{167} curve was seen to tail into a small amount of activity which decayed with approximately an 85 day half-life. This could have been either 85 day Tm^{168} , 129 day Tm^{170} , or a mixture. Assuming that it was all 85 day Tm^{168} and that this nuclide has the same counting efficiency as Tm^{167} , the cross section for Tm^{168} was calculated to be less than 2 percent as large as that for Tm^{167} . It should be noted



MU-7386

Figure 6. Gamma spectrum of Tm^{167} .

that Tm^{168} is a shielded nuclide and may be formed only directly while Tm^{167} lies at the end of a chain of relatively short-lived activities.

Ytterbium:--A 62 hour Yb^{166} and 32 day Yb^{169} were the only neutron deficient ytterbium activities reported when the rare earth program was begun. The gross ytterbium fraction separated in these bombardments gave a decay curve which could be separated into five components: an initial 74 minute activity, growth of a daughter into a parent having a 57.4 hour half-life, a 9.6 day line, and a 32 day tail. A copy of this decay curve is shown in Figure 7. Time-of-flight separation of the gross ytterbium activity showed the 57 hour activity to be Yb^{166} with the 7.7 hour Tm^{166} daughter growing in. The 32 day activity was separated at mass 169.

The short-lived 74 minute activity decayed too rapidly to allow isotopic separation to be carried out. In an experiment where ytterbium was chemically separated immediately after bombardment, allowed to decay for 24 hours, and a second ytterbium-thulium column separation run, the only activities present in the thulium fraction were 7.7 hour Tm^{166} and 9.6 day Tm^{167} . On the basis of this milking, the 74 minute activity is assigned to Yb^{167} . No gamma data were obtained on this nuclide because of the presence of so much other activity. Analysis of data taken on a crude beta spectrometer showed a positron of 2.4 ± 0.2 Mev to be present and that it decayed with approximately a 70 minute half-life. No abundances were obtained on this positron.

Gamma spectra taken on Yb^{166} showed gamma rays of 80, 112, 140, 180, 670, 800, and 1320 kev as well as the 47 kev x-rays to be present in the ytterbium-thulium equilibrium mixture.

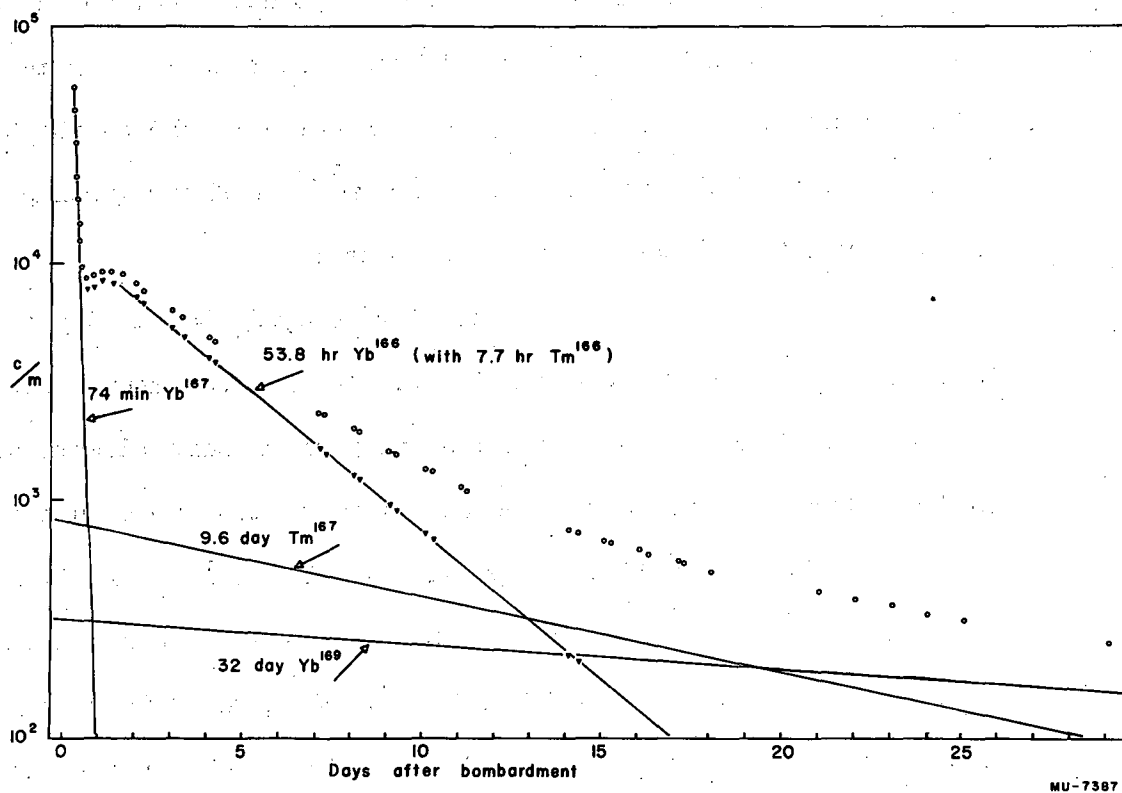


Figure 7. Gross ytterbium decay curve.

Lutetium:--The gross decay curve of the lutetium fraction could be resolved into activities having half-lives of 1.7 days, approximately 7.5 days, 32 days, and a small amount of a long-lived tail. Attempts to separate these activities on the time-of-flight isotope separator were unsuccessful. In calculating cross sections for the lutetium isotopes, published data on the half-lives were used. The 1.7 day activity was assumed to be Lu^{170} .

The 8.5 day and 6.7 day half-lives have been reported for Lu^{171} and Lu^{172} , respectively, but activities with half-lives as similar as these could not be resolved in the gross decay curve. Since both of these isotopes are essentially shielded nuclides, their formation cross sections are of particular interest. In order to get an approximate value for their cross sections, their combined decay curve was treated as a single activity having a half-life of 7.5 days and the resulting cross section value divided in two. This is admittedly only an approximation to the actual cross section but since the two nuclides have adjacent masses it should not be too far off.

Presence of a 32 day activity is somewhat puzzling. Since the lutetium-ytterbium separation is a difficult one, it is possible that the activity is an impurity of 32 day Yb^{169} . In these column runs, however, the lutetium and ytterbium peaks were well separated, and since only the leading edge of the lutetium peak was used, the contamination due to ytterbium may be considered negligible. It seems more probable that 32 day Yb^{169} is growing into the lutetium fraction as a daughter activity of Lu^{169} . From the relative magnitude of the 32

day and 1.6 day activities, the 1.6 day activity could be the Lu¹⁶⁹ parent. Further work will have to be done before any more definite mass assignments can be made.

The very long-lived activities in the tail of the decay curve could have been 1.6 year Lu¹⁷¹, 1.4 year Lu¹⁷³, 165 day Lu¹⁷⁴, or a mixture of these activities. Samples from which cross sections were calculated have not been followed long enough for accurate identification of these species so their cross sections are not included in the tabulated data.

Hafnium:--Five active neutron deficient isotopes of hafnium have been reported: 1.9 hour Hf¹⁷⁰, 16 hour Hf¹⁷¹, ~5 year Hf¹⁷², 24 hour Hf¹⁷³, and 70 day Hf¹⁷⁴. In the gross decay curve of the hafnium fraction activities having half-lives of ~70 days, 8.5 days, 44 ± 2 hours, and 12 ± 1 hours were separated. Analysis of the gamma spectra showed gamma rays of 122 ± 10, 275 ± 10 kev and 55 kev x-rays to be associated with the 44 hour activity while a gamma ray of 175 ± 10 kev seems to be present in the 12 hour activity.

The 12 hour activity is presumably the 16 hour Hf¹⁷¹ reported while the 8.5 day activity is its Lu¹⁷¹ daughter. The short-lived half-life was obtained after resolution of three other components of the gross decay curve so that this half-life would be subject to greater errors than any of the others. All of the hafnium samples gave the same half-life within the errors reported, however, so a value of 12 hours was used in the Hf¹⁷¹ cross section calculations.

The 44 hour activity is more puzzling. It is uncomfortably close to the 52.8 hour half-life reported for Ta¹⁷⁷ and makes one suspect

that tantalum may have carried through the chemistry. If this were true, however, the 8 hour tantalum activities should also have been seen, but in approximately thirty times the abundance of Ta^{177} . No evidence was seen of any 8 hour component. Further, if a mixture of 24 hour and 52.8 hour activities were present, even in comparable abundances, the decay curve would show a decided bend. This was not the case; the resolved 44 hour component was a straight line over approximately five half-lives. Although further bombardments will have to be run to clear up this matter, for the purpose of these experiments, it was concluded that the 44 hour activity was actually Hf^{173} and cross sections were calculated on that basis.

Tantalum:--Seven activities of neutron deficient tantalum isotopes have been reported in the literature. The gross decay curves of tantalum samples separated immediately after bombardment could be resolved into activities having half-lives of approximately 100 minutes, 8 hours, 2.2 days, and a small amount of a long-lived activity which had a half-life greater than 50 days. No detailed gamma spectra for these nuclides were available for identification. In the cross section calculations the 2.2 day activity was assumed to be 2.2 day Ta^{177} and the 100 minute activity Ta^{178} . The 8 hour line was undoubtedly a mixture of 8.0 hour Ta^{176} and 8.1 hour Ta^{180} . Since these could not be separated on the gross decay curve their combined total cross section is tabulated. Decay of the long-lived tail has not been followed long enough to identify the 2 year half-life reported for Ta^{179} so data for that nuclide have not been included in the cross section figures.

Tungsten:--Five active neutron deficient tungsten isotopes have been reported, and four of them have active tantalum daughters. In the tungsten fraction decay curves activities having half-lives of 21.5 days, 53 hours, 8 hours, and approximately 130 minutes were resolved. The 130 minute activity was probably a mixture of W^{176} and W^{177} . In the calculations, cross sections for these nuclides were based on the abundances of their 8.0 hour Ta^{176} and 53 hour Ta^{177} daughter activities.

The 21.5 day activity was assumed to be the 21 day W^{178} with its 9.35 minute Ta^{178} daughter in equilibrium.

No evidence was seen of the 140 day W^{181} , although the tungsten decay curve was followed as close to background as was practicable. In the gross decay curve a 140 day activity could not have been present in an abundance ratio greater than 10 counts to 2000 counts of the 21.5 day W^{178} .

IV. RESULTS AND DISCUSSION

Cross sections for spallation and fission fragments formed in 340 Mev bombardments of tantalum are presented in Table I. Cross sections for individual nuclides represent average values taken from a series of bombardments and are calculated on the basis of a 10.0 mb cross section for the reaction $Al^{27}(p,3pn)Na^{24}$ in the aluminum monitor foils.³⁷

The average error of these cross sections will depend on the type of decay involved. For neutron excess beta emitting activities, cross

Table I
Cross Sections

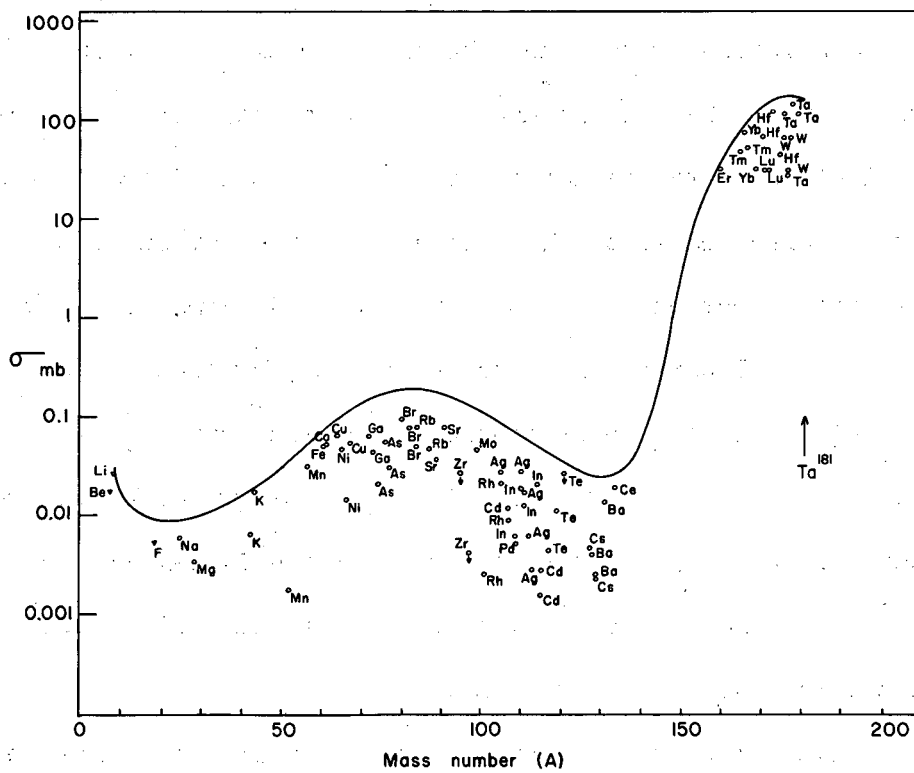
Nuclide	Cross Section (mb)	Nuclide	Cross Section (mb)
Na ²⁴	0.006	Rb ⁸⁶	0.047
Mg ²⁸	0.0035	Sr ⁸⁹	0.036
K ⁴²	0.0066	Sr ⁹¹	0.016
K ⁴³	0.017	Zr ⁹⁵	0.027
Mn ⁵²	0.0018	Zr ⁹⁷	0.0042
Mn ⁵⁶	0.033	Mo ⁹⁹	0.046
Fe ⁵⁹	0.050	Ru ⁹⁷	0.0015
Co ⁶¹	0.054	Ru ¹⁰³	0.032
Ni ⁶⁵	0.038	Ru ¹⁰⁵	0.0032
Ni ⁶⁶	0.015	Rh ¹⁰¹	*0.0023
Cu ⁶⁴	0.065	Rh ¹⁰⁵	0.022
Cu ⁶⁷	0.054	Rh ^{107m}	(0.009)
Ga ⁷²	0.064	Pd ¹⁰⁹	0.0052
Ga ⁷³	0.044	Ag ¹⁰⁵	*0.027
As ⁷⁴	0.021	Ag ^{110m}	0.029
As ⁷⁶	0.056	Ag ¹¹¹	0.018
As ⁷⁷	0.030	Ag ¹¹²	0.0064
Br ^{80m}	0.095	Ag ¹¹³	0.0029
Br ⁸²	0.080	Cd ¹⁰⁷	0.012
Br ⁸³	0.050	Cd ¹¹⁵	0.0016
Rb ⁸⁴	0.078	Cd ^{115m}	0.0027

Table I, cont.

Nuclide	Cross Section (mb)	Nuclide	Cross Section (mb)
In ¹⁰⁹	*0.0062	Tm ¹⁶⁵	48.6
In ^{110m}	0.019	Tm ¹⁶⁷	50.7
In ¹¹¹	0.013	Yb ¹⁶⁶	76
In ^{114m}	0.021	Yb ¹⁶⁹	32.6
Te ¹¹⁷	*0.0045	Lu ¹⁷⁰	218
Te ¹¹⁹	*0.011	Lu ^{171,172}	63.7
Te ¹²¹	0.028	Hf ¹⁷¹	67
Cs ¹²⁷	*0.0047	Hf ¹⁷³	130
Cs ¹²⁹	*0.0022	Hf ¹⁷⁵	45
Ba ¹²⁸	0.0041	Ta ¹⁷⁷	27
Ba ¹²⁹	*0.0025	Ta ¹⁷⁸	152
Ba ¹³¹	0.013	Ta ^{176,180}	265
Ce ¹³⁴	0.019	W ¹⁷⁶	65
Ce ¹³⁵	0.22	W ¹⁷⁷	30
Er ¹⁶⁰	31.3	W ¹⁷⁸	65

sections should be reproducible to ± 5 percent. In view of the large number of corrections involved in the calculations, however, an average error of no better than ± 15 percent can be claimed. For neutron deficient isotopes whose decay schemes, abundances of positrons and gamma rays, and conversion coefficients are known accurately, this same limit of error should apply. For those nuclides whose decay schemes are not accurately known, and about which assumptions were made, the cross sections will obviously be no more accurate than the assumptions. Cross sections for nuclides in this last category are marked with (*) in Table I and must be regarded only as approximations. Neutron deficient electron capture nuclides whose cross sections are based on x-ray and gamma counting through absorbers will not be affected too greatly by lack of information concerning detailed decay schemes. Counting efficiency of a mixture of gamma and x-rays differing widely in energy can be somewhat uncertain when samples are counted in the Geiger-Müller counter, however, so that an accuracy of no better than ± 25 percent may be claimed for samples counted in this way.

A plot of cross section versus mass number for those nuclides in Table I is shown in Figure 8. In addition, cross sections for Be^7 , Li^8 , and F^{18} which were obtained by interpolation in curves reported by Marquez³⁸ are included for reference. Several features of this plot are apparent even at first glance. First, cross sections for fragments in the fission region differ from those in the spallation region by factors as high as 10^4 . Second, although the fission cross sections are low, a fission peak is discernable. Third, although



MU-7388

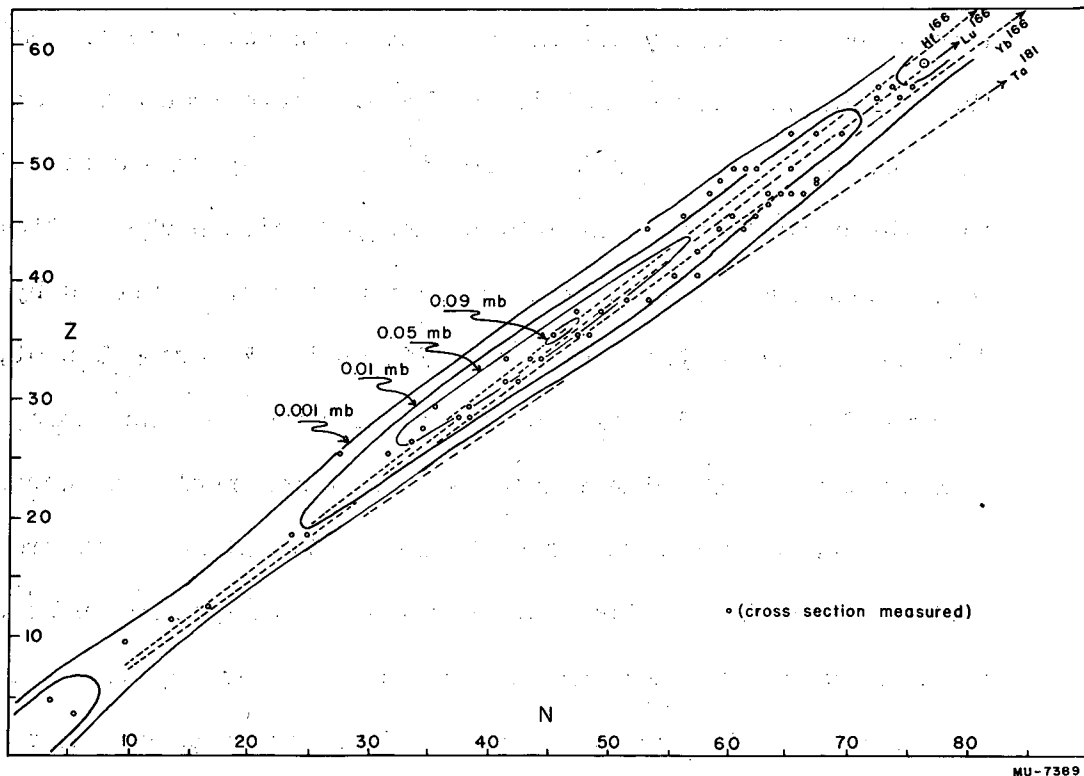
Figure 8. The distribution of spallation and fission products as a function of mass. Solid line depicts the total chain yield curve obtained by integration of cross sections in Figure 9.

there is a fission peak, it is very small and relatively flat so that fragments due to fission may be spread over a very wide range of atomic numbers.

When the cross sections are plotted on a "chart of nuclides," i.e., atomic number versus neutron number for all nuclides, this spread out quality of the fission peak becomes much more apparent. Maximum cross sections for a given mass lie fairly close to the main line of beta stability for all elements from sodium to indium but these cross sections do not differ by much more than a factor of ten. This compares with "peak to valley"* ratios of approximately 10^3 for both the bismuth and uranium high energy fission peaks. Attempts to make a detailed analysis of this fission peak are hampered by the fact that it is so broad and low. If, on the Z versus N plot, a line is drawn between all nuclides having the same cross sections, reasonable interpolation being made between adjacent nuclides, curves such as those shown in Figure 9 are obtained. If estimates of cross sections of stable nuclides are now made by interpolation between these isobarn lines and summed for each mass number, the solid curve of Figure 8 may be drawn. This line will then represent the total chain yield at each mass number.

Cross sections for nuclides in the spallation region of tantalum are shown in the Z versus N chart of Figure 10. Masses for which the

*The ratio of the total chain yield cross sections at the fission peak to those at the minimum in the region between fission and spallation.



MU-7389

Figure 9. Cross section contour plot of the fission area.

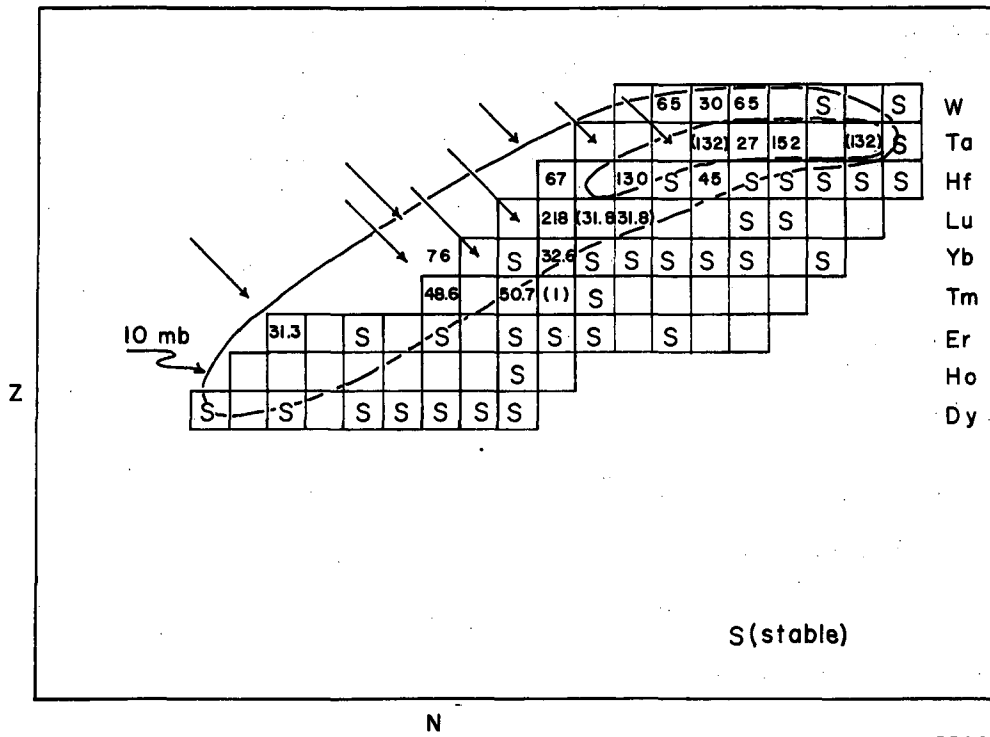


Figure 10. Cross sections in the spallation region of tantalum.

plotted cross section represents total yield for the given nuclide plus all of its precursors are designated by arrows pointing down the chain. In the case of Lu¹⁷¹⁺¹⁷² and Ta¹⁷⁶⁺¹⁸⁰ the summed cross section listed in Table I has been divided by two and plotted in brackets.

Discussion

Inspection of these figures leads to several very interesting conclusions. The peak of the fission curve in Figure 8 lies at approximately mass number 83, indicating a "most probable fissioning nucleus" having a mass of 166. From the contour lines of Figure 9 it is not possible to say that the peak cross section of mass 83 lies at atomic number 35 or 36, either one of which seems probable. Biller, in his work on bismuth,¹⁴ came to the conclusion that the peaks of his chain yields fell on a straight line having the same neutron to proton ratio as his most probable fissioning nucleus. Lines drawn with the neutron to proton ratio for Hf₇₂¹⁶⁶, Lu₇₁¹⁶⁶, and Yb₇₀¹⁶⁶ are included in Figure 9. From the fit of these lines to the isobarns plotted it is apparent that either Hf¹⁶⁶ or Lu¹⁶⁶ is equally possible as the most probable fissioning nucleus while Yb¹⁶⁶ has too low an atomic number to fit the data. Thus it may be said that the most probable fissioning process is one in which the Ta¹⁸¹ target atom loses sixteen nucleons before the fission process takes place (counting the incident proton as being emitted also), and that these nucleons are boiled off in the ratio of 2.5 protons to 13.5 neutrons. Although there undoubtedly may be some leeway in the choice of the most probable

fissioning nucleus, these data are not inconsistent with Biller's results on bismuth, where two protons and 19 neutrons must be boiled off to give the most probable fissioning nucleus, or with the results of Folger with uranium, where two protons and approximately 20 neutrons are emitted.

From the shape of the total chain yield versus mass number curve of Figure 8 three separate areas may be delineated: first, the area of very light masses (and probably relatively high cross sections) which represent small fragments emitted as part of the spallation process; second, the fission area corresponding to fragments having comparable sizes, or sizes larger than those normally considered as being involved in spallation reactions; and third, the area involving end products of spallation reactions in which only relatively small particles are ejected from the excited nucleus. It is evident that these areas are not very sharply defined for this type of bombardment; one cannot say precisely where the spallation process ends and fission begins, or where fission ends and the spallation fragments begin. Actually, it is not likely that there is a sharp dividing line; the curves undoubtedly overlap to some extent. For the sake of argument, however, let us take the area under the total chain yield curve between the two minima in Figure 8 (mass 20 through 132 inclusive) as a measure of the total fission cross section. Upon integrating this portion of the curve and dividing by two for a binary fission process the total fission cross section obtained for 340 Mev protons on tantalum is 4.1 ± 1.5 mb. This compares with 2000 mb for uranium,¹⁵ 239 ± 30 mb

for bismuth,¹⁴ and approximately 10^{-1} - 10^{-2} mb for silver¹³ under the same bombardment conditions.

Note should be taken of trends that are apparent in the distribution of fission products as the atomic number of the target material is increased. In silver, and to a lesser extent copper, indications are that in the fission region no symmetrical fission peak is detectable. Fission data for these elements are meager, (i.e., five measured cross sections between mass 24 and mass 56 in the silver bombardments) so that no detailed information concerning the fission region is available. Even if such information were known, however, it seems probable that the indefinite extent of the spallation process would tend to make interpretation of the fission data difficult. These total reaction cross section curves may be considered as a superposition of spallation and fission cross section components and if spallation extends into the fission area and effect will be to raise the "wings" of the fission curve, i.e., make it appear as though asymmetric fission were more probable than is actually the case. About all that can be done in the lighter elements is to set an upper limit to the total fission cross section, without any knowledge about the distribution of the fission fragments.

This "contamination" of the fission peak by products which may be due to spallation is negligible for bismuth and uranium. Here fission is a predominant reaction and the fission cross section peak height is such that the ratio between cross sections at the fission peak and those at the minimum in the region between fission and spallation is roughly 10^3 . For these elements the conclusion has been drawn that

binary fission into roughly equal sized fragments is by far the most probable type of fission reaction.

The tantalum fission data seem to lie between these two extremes. From the shape of the total chain yield versus mass curve in Figure 8 we may consider that the fission region extends roughly from mass 20 to mass 132. There will be overlapping between spallation and fission curves at the two extremes of this region, of course, but it is difficult to see how spallation, i.e., emission of a long series of small particles, will extend far enough into the fission region to change the shape of the fission curve significantly. It would appear, therefore, that the spread-out quality of the tantalum fission peak is real and that asymmetric fission is relatively more highly probable than in either bismuth or uranium. As a measure of this tendency toward asymmetric fission, let us compare the ratio of the cross section for symmetrical fission to that for a process in which the fissioning nucleus splits into fragments having masses in the ratio 70:30. In uranium¹⁵ the 50:50 split is approximately 47 times more probable than the 70:30 process. In bismuth¹⁴ the ratio is about 88; and in tantalum, 5. These numbers are made somewhat uncertain by the steep slopes of the fission curves for bismuth and uranium, but they do indicate a trend which suggests an extension of the line of reasoning used to explain the change in shape of the double humped thermal neutron uranium fission peak as the energy of the bombarding particle is increased. Here the nuclear shell effects which probably contribute to asymmetric fission with thermal neutrons are overpowered, as it were, by larger nuclear excitation energies and symmetrical

fission becomes favored. The fact that the above ratio is lower for uranium than for bismuth may indicate that the low energy asymmetric fission process is still important enough with 340 Mev protons to broaden the uranium fission peak somewhat. This interpretation seems reasonable in view of the fact that such a wide range of excitation energies may be imparted to the target nucleus and that even in uranium nuclei excited to about 40 Mev the peaks for asymmetric fission may be seen.

No similar asymmetric fission process is known for tantalum, however, which could explain the fact that the 70:30 fission process is 17 times more probable in tantalum than in bismuth. The small magnitude of the tantalum total fission cross section and the calculated height of the potential barrier indicate that a larger excitation energy is required to get tantalum into a fissionable state than is necessary for either bismuth or uranium. From the width of the fission peak for tantalum, it may be inferred that these very high excitation energies tend to destroy the fissioning nuclides' preference for roughly symmetrical fission.

The question naturally arises as to why these nuclides split at all, even in the region of the most probable fissioning nucleus. It seems unlikely that there is anything unique about Hf^{166} or Lu^{166} that would make them fission more than other nuclei in that portion of the periodic table. If lutetium or ytterbium were bombarded instead of tantalum one would not expect Hf^{166} or Lu^{166} to be the "most probable fissioning nucleus" for those elements. No major closed shells are present to affect nuclear stability appreciably and with these large

excitation energies one would not expect minor shell configurations to play a significant part. The "major fission products" (placed in quotes because they are not much more major than the minor fission products) have three or four neutrons less than the closed shell at fifty neutrons so that if neutron evaporation occurs after fission the closed neutron shell may play a significant part in increasing the fission probability. There is no evidence that this shell effect plays an important part in the bismuth or uranium fission processes, however, so it does not seem too probable that it is a decisive factor in tantalum.

Attempts to interpret fission phenomena from a theoretical point of view have not been entirely successful, particularly for the high energy reactions. A comprehensive treatment of the fission process in terms of the liquid drop model has been presented by Bohr and Wheeler⁴² and later improved by Frankel and Metropolis.³⁹ Here the nucleus is regarded as a spherical drop of incompressible liquid with surface tension arising from attractive forces between nucleons. By application of appropriate forces this spherical drop may be excited into various modes of vibration. If the excitation energy is large enough these vibrations will deform the sphere into an ellipsoidal, or, finally, into a dumbbell shaped nucleus in which the stability is reduced and fission may occur. Although the liquid drop model does not predict the observed asymmetry of low energy fission, it has been used to explain some aspects of the fission process, i.e., the limit of stability of nuclei against fission, the threshold energy for fission, etc.

For a number of nuclides it has been shown empirically⁴⁰ that the rate of spontaneous fission bears some relationship to the "fissionability parameter" Z^2/A from the liquid drop model. These data apply to unexcited nuclei, of course, but for this type of reaction a Z^2/A value of approximately 47 is needed for "instantaneous fission," i.e., a fission half-life of on the order of 10^{-20} seconds. For Hf^{166} or Lu^{166} in the tantalum bombardments, where the rate of fission must be fast to compete with spallation, the Z^2/A values are 31.2 and 30.4, respectively. Application of the Z^2/A criterion to highly excited nuclei is probably not too justifiable but the tantalum data indicate that these values are far too low for the Z^2/A of the unexcited nucleus to play a large part in determining the fission probability.

If the hypothesis of nuclear transparency suggested by Serber⁴¹ is essentially correct, incident protons having 340 Mev of energy may impart a very wide range of excitation energies to a tantalum target nucleus. The present data suggest that this excitation energy may be dissipated in several different ways. Each excited nucleus may lose energy by emission of gamma rays, by emission of nucleons, either charged or uncharged, in a spallation type reaction, or by fission into two or more large fragments. For the lower excitation energies the spallation data of Figure 10 indicate that gamma ray emission and neutron boil-off (protons to a lesser degree) are the only important competing reactions. The fission process does not seem to be significant. At higher excitation energies, after a fairly large number of neutrons and possibly one or two protons have been evaporated, emission

of charged particles and fission both become increasingly important. Even under these circumstances, however, it is interesting to note that the fission process does not play a very large part. Let us assume for the sake of argument that all of the spallation products below mass number 166 had to be formed by a spallation process in which they passed through mass 166, i.e., that spallation proceeds by emission of single nucleons, at least through mass number 166. Integration of the spallation cross section curve below mass number 166 and comparison with the total fission cross section should then give an indication of the relative probabilities for spallation and fission for those tantalum atoms which had at least sufficient excitation energy to evaporate sixteen nucleons. Treatment in this manner shows a total spallation cross section of about 600 mb below mass 166 as against a fission cross section of 4.1 mb. In view of the fact that one must actually consider a region of fissioning nuclei rather than a single mass, and that this region should extend to masses higher than 166, this ratio must be regarded as only very approximate. As an order of magnitude, however, it shows that even when tantalum nuclei receive enough initial excitation energy to reach the "region of most probable fission" less than 1 percent of the nuclides actually do split; the rest go on to dissipate their energy by spallation.

The spallation cross section data of Figure 10 indicate that the highest cross sections are for those reactions in which the incident proton is not captured and only a few neutrons are evaporated. The probability of a proton being emitted with these first neutrons could not be determined because of the stability of hafnium isotopes in this

region, but from the magnitude of the cross section for the production of Hf^{175} it may be inferred that this probability is small compared to neutron evaporation. These data also indicate that spallation of as many as 21 nucleons has a cross section lower than the maximum by only a factor of 7.

Strictly speaking, by radiochemical techniques it is possible to detect only the end products of spallation reactions and not the mechanism by which those products were formed. Thus a reaction in which four alpha particles were emitted would give the same nucleus as one in which eight deuterons or eight protons and eight neutrons were boiled off. In the tantalum spallation data some additional conclusions concerning the mode of formation of the spallation products may be inferred from a comparison of the cross sections for formation of Tm^{167} and Tm^{168} . In this case Tm^{168} is a shielded nuclide and may be formed only by spallation of five protons and nine neutrons (or combinations of these) from the target nucleus. Thulium 167, however, in addition to being formed by direct spallation of five protons and ten neutrons from tantalum, could have been formed by beta decay of members of the mass number 167 chain with higher Z; i.e., Yb^{167} , Lu^{167} , Hf^{167} , Ta^{167} , and W^{167} . Since Tm^{167} and Tm^{168} are neighboring isotopes, it is reasonable to assume that their cross sections for formation by direct spallation are comparable. In view of the fact that the observed cross section for Tm^{167} is approximately fifty times that of Tm^{168} the conclusion naturally follows that most of the observed cross section for the formation of Tm^{167} must be due to contributions of its precursors and that the major portion of the 167 chain yield lies in nuclides

having atomic numbers greater than 69. Thus a spallation process in which fifteen nucleons are emitted will, in a great majority of cases, involve emission of eight nucleons as neutrons, i.e., by a reaction of the type $Ta^{181}(p, p8n\alpha d)Yb^{167}$, or if a compound nucleus is formed, seven neutrons: $Ta^{181}(p, 7n2\alpha)Yb^{167}$. Of course, a larger number of neutrons (and a smaller number of charged particles) may be emitted to give members farther out on the mass number 167 chain.

V. ACKNOWLEDGMENTS

I wish to express my gratitude to Professor G. T. Seaborg, under whose supervision this work was done. The cooperation of Mr. J. T. Vale, Mr. L. Hauser and members of the cyclotron operating group in carrying out the many bombardments is gratefully acknowledged. Thanks are also due Mrs. Roberta Garrett for considerable assistance in counting the samples and aiding in the ion exchange assaying, and to Mrs. W. Nervik and Mrs. M. Kalm for aid in typing and preparing the final report. I wish to thank Mssrs. J. Conway, W. Tuttle, and R. McLaughlin for providing spectrographic analyses of the tantalum target material and many of the samples. The patient collaboration of Dr. M. Michel in the trying mass spectrographic identification of the rare earth activities is gratefully acknowledged. I also wish to thank Dr. P. C. Stevenson and Dr. H. Hicks for their continued interest, helpful criticism, and willing assistance during the initial portion of the research.

This work was performed under the auspices of the U. S. Atomic Energy Commission.

VI. REFERENCES

1. Engelkemeir, Freedman, Seiler, Steinberg and Winsberg, Radio-chemical Studies: The Fission Products (McGraw-Hill Book Co., Inc., New York, 1951), National Nuclear Energy Series, Plutonium Project Record, Div. IV-9, Paper 204, pp. 1331-1333.
2. E. P. Steinberg and M. S. Freedman, Ibid., Paper 219, pp. 1378-1390.
3. A. Turkevich and J. B. Niday, Phys. Rev. 84, 52 (1951).
4. R. W. Spence, Atomic Energy Commission Declassified Report AECD-2625 (June 1949).
5. A. J. Newton, Phys. Rev. 75, 17 (1949).
6. P. R. O'Connor and G. T. Seaborg, Phys. Rev. 74, 1189 (1948).
7. R. H. Goeckermann and I. Perlman, Phys. Rev. 73, 1127 (1948).
8. R. E. Batzel and G. T. Seaborg, Phys. Rev. 79, 528 (1950).
9. Ibid., 82, 607 (1951).
10. G. Rudstam and P. C. Stevenson, private communication.
11. B. Haldar, private communication (1952).
12. W. J. Worthington, University of California Radiation Laboratory Report UCRL-1627 (January 1952).
13. P. Kofstad, University of California Radiation Laboratory Report UCRL-2265 (June 1953).
14. W. F. Biller, University of California Radiation Laboratory Report UCRL-2067 (December 1952).
15. R. L. Folger, University of California Radiation Laboratory Report UCRL-1195 (May 1951).

16. M. Lindner and R. N. Osborne, private communication (1954).
17. Si-Chang Fung, University of California Radiation Laboratory Report UCRL-1465 (August 1951).
18. Hollander, Perlman, and Seaborg, Revs. Modern Phys. 25, 469 (1953).
19. M. Studier and R. James, unpublished data.
20. P. W. Maguire and G. D. O'Kelley, California Research and Development Corporation Report MTA-40 (September 1953).
21. Kahn and Lyon, Nucleonics 11, No. 11, 61 (November 1953).
22. L. R. Zumwalt, Atomic Energy Commission Declassified Report MDDC-1346 (September 1947).
23. P. B. Burt, Nucleonics, page 28 (August 1949).
24. H. H. Seliger, Phys. Rev. 88, 408 (1952).
25. Seelmann-Eggebert, Nature 31, 201 (1943).
26. W. Nervik and P. C. Stevenson, Nucleonics 10, 18 (1952).
27. General Electric Chart of the Nuclides, Knolls Atomic Power Laboratory, Revised to November 1952.
28. H. Mathur, private communication (1954).
29. Wapstra, Versta, and Boelhouwer, Physica, Deel XIX, No. 1-2, 138 (1953).
30. M. Lindner, private communication.
31. R. W. Fink and E. O. Wiig, Phys. Rev. 91, 194 (1953).
32. B. J. Stover, Phys. Rev. 81, 8 (1951).
33. M. C. Michel, University of California Radiation Laboratory Report UCRL-2267 (1953).
34. T. H. Handley and E. L. Olson, Oak Ridge National Laboratory, private communication (September 1953).

35. T. H. Handley, Oak Ridge National Laboratory, private communication (January 1954).
36. T. H. Handley and E. L. Olson, Phys. Rev. 92, 1260 (1953).
37. P. C. Stevenson, private communication.
38. Luis Marquez, Phys. Rev. 86, 405 (1952).
39. S. Frankel and N. Metropolis, Phys. Rev. 72, 914 (1947).
40. G. T. Seaborg, Phys. Rev. 85, 157 (1952).
41. R. Serber, Phys. Rev. 72, 1114 (1947).
42. N. Bohr and J. A. Wheeler, Phys. Rev. 56, 426 (1939).